Thesis

On

STRESS ANALYSIS IN A FUNCTIONALLY GRADED ROTATING DISC OF NON-UNIFORM THICKNESS UNDER THERMAL LOADING

Submitted in partial fulfilment of the requirements for the award of degree of

Masters of Engineering

IN

PRODUCTION AND INDUSTRIAL ENGINEERING

Submitted By

RUPINDER SINGH

Roll No. 801182022

Under the Guidance of

Mr. KISHORE KHANNA

Assistant Professor

MECHANICAL ENGINEERING DEPARTMENT

THAPAR UNIVERSITY, PATIALA-147004, PUNJAB

July, 2013

CERTIFICATE

This is to certify that the work in this thesis report entitled **"STRESS ANALYSIS IN A FUNCTIONALLY GRADED ROTATING DISC OF NON-UNIFORM THICKNESS UNDER THERMAL LOADING"** submitted in partial fulfilment of requirement for the award of **Masters of Engineering Degree** in **Production and Industrial Engineering** in Mechanical Engineering Department of Thapar University, Patiala, is an authentic record of work carried out by me under the guidance of **Mr. Kishore Khanna,** Assistant Professor, Mechanical Engineering Department, Thapar University, Patiala.

The matter embodied in this report has not been submitted in part or full to any other university or institute for the award of any degree.

Rupinder Singh

Dated: 15/7/2013

This is to certify that the above declaration made by the student concerned is correct to the best of my knowledge and belief.

Mr. Kishore Khanna
Assistant Professor,
Mechanical Engineering Department,
Thapar University, Patiala.

Countersigned By:

Dr. Ajay Batish
Professor & Head MED,
Thapar University, Patiala.

Dr. S.K. Mohapatra
Dean Academics Affairs,
Thapar University, Pataila.

AKNOWLEDGEMENT

I express my deep sense of gratitude and a very sincere thanks to my guide, **Mr. Kishore Khanna**, Assistant Professor, **Mechanical Engineering Department, Thapar University, Patiala** for his indefatigable guidance and full support which helped me in the accomplishment of this research work. I am highly indebted to him for his painstaking efforts and cooperation all the time during the period of work.

I am highly thankful to **Mr. Manish Garg** for his invaluable suggestions and continuous support.

I am also thankful to all my friends, who devoted their valuable time and helped me in all possible ways towards successful completion of my thesis work.

I do not find enough words with which I can express my feeling of thanks to the head of department, entire faculty and staff of **Mechanical Engineering Department, Thapar University,** for their help, inspiration and moral support, which went a long way in successful completion of my thesis.

At last but most important I am highly indebted to my dear parents for their love, support and trust.

RUPINDER SINGH

ABSTRACT

In the present thesis work, the stress analysis has been carried out in a functionally graded disc of non-uniform thickness, rotating at constant angular velocity and subjected to internal pressure and thermal loads by using infinitesimal deformation theory of elasticity. For the purpose of investigation, three discs, made of composite containing silicon carbide particles (SiC_p) in a matrix of pure aluminium, with varying particle content along the radius are considered. The material of the disc is assumed to be isotropic with constant Poisson's ratio (v). The Young's modulus of elasticity (E), density (ρ) and thermal expansion coefficient (α), are varying along the radial direction. For this purpose, power law functions are used. The influence of particle content and basic factors such as, thickness gradient (k), grading index (n), thermal loading and internal pressure (p_i) on stresses, strain rates and displacement in rotating FGM disc have been investigated.

TABLE OF CONTENTS

CONTENTS **PAGE NO.**

LIST OF FIGURES

LIST OF TABLES

CHAPTER 1
INTRODUCTION

1.1 COMPOSITE MATERIALS

Composite is a structural material which consists of combining two or more constituents. The constituents are combined at a macroscopic level and are not soluble in each other. One constituent is called reinforcing phase and the one which it is embedded is called matrix. The reinforcing phase may be in the form of fibers, particles, or flakes. The matrix phase material is generally continuous [32]. Composites are mainly divided into two types:

(i) Natural Composites (*Existing in nature*)

(ii) Synthetic Composites (*Man made*)

Natural Composites: Wood, Figure 1.1, is a natural composite of cellulose fibers in a matrix of lignin.

Figure 1.1 Natural composites [34].

Synthetic Components: An example of a synthetic composite, Figure 1.2, is concrete which is structural composite obtained by combining (through mixing) cement (the matrix, i.e., the binder, obtained by a reaction known as hydration between cement and water), sand (fine aggregate), gravel (coarse aggregate), and optionally other ingredients that are known as admixtures [33].

Figure 1.2 Synthetic composites [35].

1.1.1 Classification of composites

Composites, Figure 1.3, are classified by the geometry of the reinforcement [32] i.e. fiber, particulate and flake or by the type of matrix i.e. metal, ceramic, carbon, and polymer.

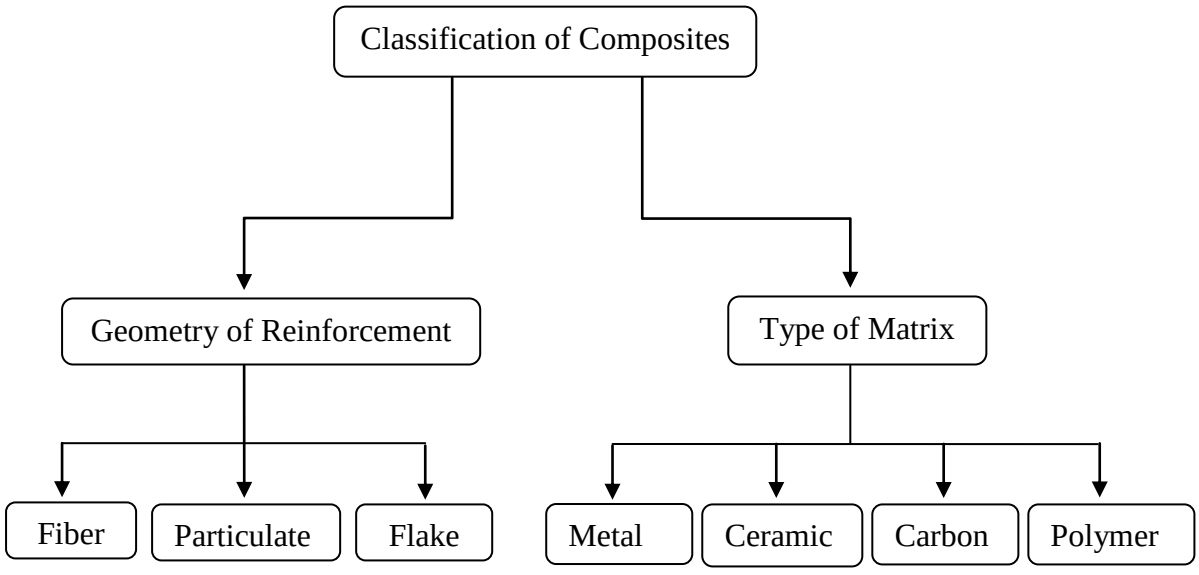

Figure 1.3 Classifications of composites.

Classification of synthetic composites [32] on the basis of reinforcement:

(i) Fibers

(ii) Particulate

(iii) Flake

Fibers: Fiber composites, Figure 1.4, consist of matrices reinforced by short (discontinuous) or long (continuous) fibers. Fibers are generally anisotropy and examples include carbon and aramids. Examples of matrices are resins such as epoxy, metals such as aluminium, and ceramics such as calcium alumino silicate.

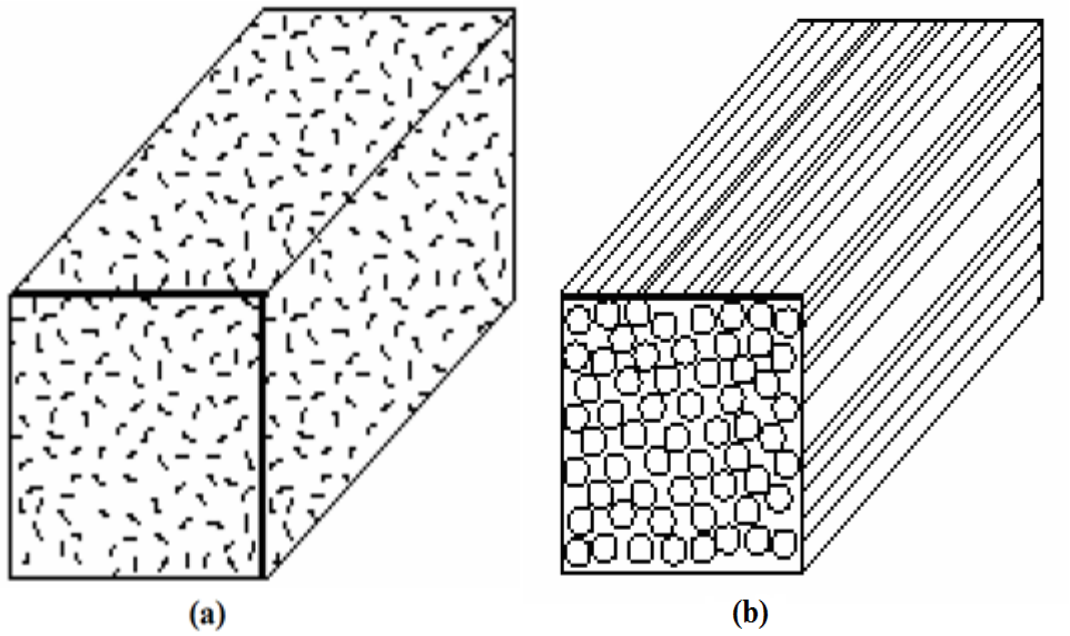

Figure 1.4 Fiber as reinforcement (a) Random fiber (short fiber) and (b) Continuous fiber (long fiber) [36].

Particulate: Particulate composites, Figure 1.5, consist of particles immersed in matrices such as ceramics and alloys. They are usually isotropic since the particles are added randomly. Particulate composites have advantages such as improved strength, increase operating temperature etc. Examples include use of silicon carbide particles in aluminium, aluminium particles in rubber and sand, gravel and cement to make concrete.

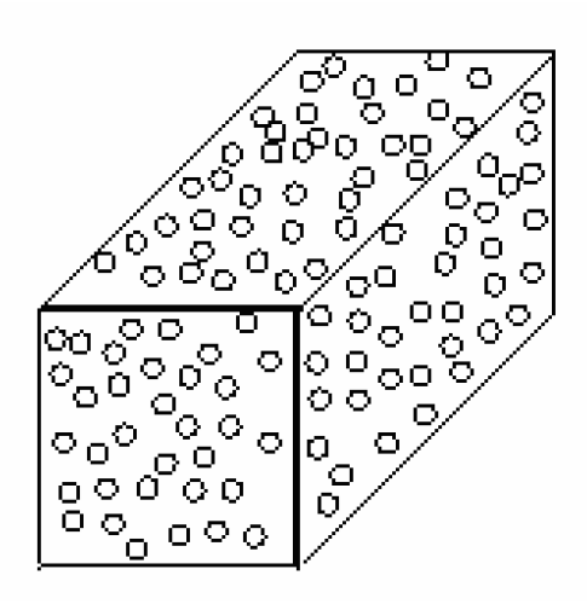

Figure 1.5 Particulate as the reinforcement [36].

Flake: Flake composites, Figure 1.6, consist of flat reinforcement in matrices. Typical flake materials are glass, mica, aluminium, and silver. Whisker composites provide advantages such as higher strength and low cost. However, whiskers cannot be oriented easily and only a limited number of materials are available of use.

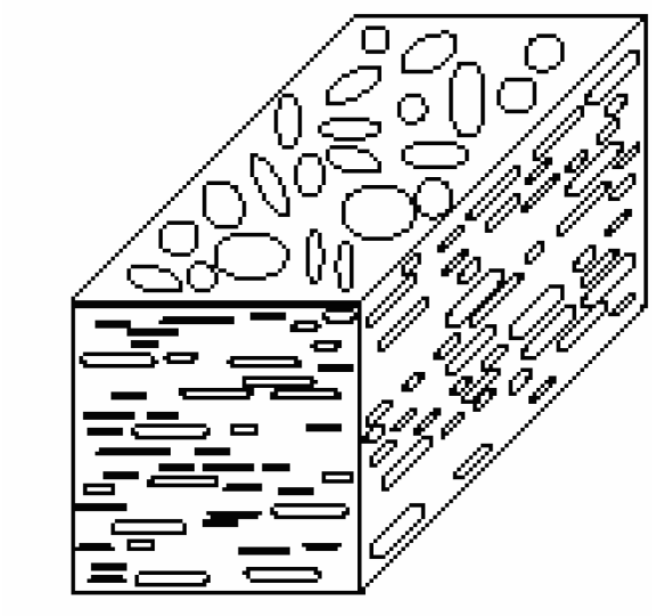

Figure 1.6 Flake as the reinforcement [36].

Classification of synthetic composites [32] on the basis of matrix:

(i) Metal Matrix Composites

(ii) Ceramic Matrix Composites

(iii) Carbon Matrix Composites

(iv) Polymer Matrix Composites

Metal Matrix Composites: Metal matrix composites (MMC) are those which have a metal as matrix such as aluminium, magnesium and titanium. Metals are mainly reinforced to decrease and increase their properties to suit the need of design [32].

Ceramic Matrix Composites: Ceramic matrix composites (CMC) are a subgroup of composite materials as well as a subgroup of technical ceramics. CMC consist of ceramic fibers embedded in a ceramic matrix, thus forming a ceramic fiber reinforced ceramic (CFRC) material [32]. The fiber can be short or continuous. Ceramic matrix composites are superior to carbon matrix composites in terms of oxidation resistance, but CMC are not as well developed as carbon matrix composites [33].

Carbon Matrix Composites: Carbon fiber reinforced polymer [32] is a very strong and light fiber reinforced polymer which contain carbon fibers. Carbon martrix composite [33] are important for lightweight structures and components but they are relatively expensive due to high cost.

Polymer-Matrix composites: Polymer matrix composites (PMC) can be classified according whether the matrix is a thermoset or a plastic polymer. Thermoset matrix composites are traditionally more common, but thermoplastic matrix composites are currently focused of rapid development. The advantages of thermoplastic matrix composites compared to thermoset matrix composites include lower manufacturing and better performance [33].

1.2 FUNCTIONALLY GRADED MATERIALS (FGMs)

In engineering applications conventional materials like metals, alone may not survive under high temperature or thermal gradient applications [22]. The use of pure metals is little because of demand of conflicting property requirement. For example, there is no such material that is hard as well as ductile existing in nature. To solve this problem, combination

of one metal with other metal or non metal is used. This combination of materials is termed alloy or conventional alloy, gives a property that is different from parent metal. Bronze is alloy of copper and tin, was the first alloy that appears in human history. There is limit to which a material can be dissolved in a solution of another material because of thermodynamic equilibrium limit. When more quantity of the alloying material is desired, then the traditional alloying cannot be used. Another limitation of conventional alloying is when alloying two dissimilar materials with wide apart melting temperatures it becomes prohibitive to combine these materials through this process. Another method of producing materials with combination of properties is by combining materials in solid state, which is referred to as composite material [28].

Composite materials are advanced materials, made up of two or more materials combined in solid states with distinct chemical and physical properties. Composite materials offers excellent properties which are differ from the individual parent materials. Composite materials fails under extreme working conditions through a process called delamination. This can happen due to high temperature applications where two metals with different coefficient of expansion are used. To solve this problem, the concept of functionally graded materials was initiated and technologically developed in 1984 in Japan [16, 28 and 26].

Functionally Graded Materials (FGMs) belongs to a class of advanced materials in which the volume fraction of the two or more materials is varied continuously as a function of position along certain dimension of the structure. FGMs are heterogeneous composite materials in which the material properties vary continuously over changing dimension [12]. FGMs are mainly constructed to operate in high-temperature environments such as ultra-light, temperature resistant materials for space vehicles [31]. Functionally graded materials occur in nature as teeth; bones etc. and find the application in engineering devices such as steam and gas turbine rotors, turbo generator gears, clutch plates and brake discs [28 and 31]. Functionally graded material, eliminates the sharp interfaces existing in composite material which is where failure is initiated. It replaces this sharp interface with a gradient interface which produces smooth transition from one material to the next. One unique characteristics of FGM is the ability to tailor a material for specific application [28]. One of the advantages of FGMs over laminates is that there is no stress build-up at sharp material boundaries due to continuous material property variation thus eliminating potential structure integrity issues such as delamination [23].

1.2.1 Areas of application [28] of FGMs:

Following are the applications of functionally graded materials in different areas:

(i) **Aerospace:** Functionally graded materials can withstand very high thermal gradient, which makes it suitable for use in structures and space plane body, rocket engine component etc.

(ii) **Medicine:** FGM has find wide range of application in dental and orthopedic applications for teeth and bone replacement.

(iii) **Defense:** The important characteristic of functionally graded material is the ability to inhibit crack propagation. This property makes it highly useful in defense application, as a penetration resistant materials used for armour plates and bullet-proof vests.

(iv) **Energy:** FGM are used in energy conversion devices. They also provide thermal barrier and are used as protective coating on turbine blades in gas turbine engine.

(v) **Optoelectronics:** FGM also finds its application in optoelectronics as graded refractive index materials and in audio-video discs magnetic storage media.

(vi) **Other Areas:** FGMs are used in many more applications such as, cutting tool insert coating, automobile engine components, nuclear reactor components, turbine blade, heat exchanger, sensors, fire retardant doors, etc.

1.3 ROTATING DISC

In engineering, rotating discs have received a great deal of attention because of their wide range of applications in mechanical and electronic devices. The theoretical and experimental investigations of stresses on the rotating solid and annular discs have been considerable attention due to the great practical importance in mechanical engineering. Rotating discs is the part of different machineries and have extensive practical engineering applications such as in flywheels, gears, gas turbine rotors, centrifugal pumps, automotive braking system, compressors, ship propellers, computer disc drives and in many other applications [21, 23 and 15].

In most of these applications, the disc has to operate under high temperature and is simultaneously subjected to high stresses due to high speed of rotation [21]. The analyses of stresses and strains in rotating disc subjected to different boundary conditions are important

for an effective design and material usage. The boundary conditions of the disk depend on the way the disc is attached to the shaft. A disc is connected rigidly to the shaft such as, welding or shaft and rotor disc cast together a fixed free condition applies. Flywheels and gear wheels are the examples of fixed free conditions. If disc is connected to the shaft by means of splines where small axial movement is allowed, a free–free condition applies [15]. Applications of non uniform thickness discs are increasing to reduce the weight, production costs and to improve the mechanical performance, while keeping the stress distribution at a uniform level [24, 16 and 26].

CHAPTER 2
LITERATURE REVIEW

As extensive literature review on rotating disc has been carried out and discussed in the following section:

Reddy and Shrinath [1] obtained a closed form solution for elastic stresses and displacement in an anisotropic disc having variable thickness and density variation. It was concluded that when the mass density of the disc material increased radially, the stresses and displacement found lower.

Guven [2] had investigated elastic plastic stresses and radial displacement in a rotating disc of variable thickness and density for linear strain hardening material under the assumption of Tresca yield condition and the boundaries of the disk were free from radial stress. The radial stresses found lower in the disc whose density decreases radially when compared with constant density disc.

Shukla [3] studied the creep stresses in thin rotating annular disc made up of non homogeneous material by using transition theory. It was observed that the presence of non homogeneity having lesser value at the bore, reduced the stresses and angular velocity required for steady state creep as compared to the homogeneous disc. Higher value of non homogeneity at the bore than the rim increased the magnitude of angular velocity and creep stresses significantly and increased the possibility of a facture in the vicinity of the bore.

Horgan and Chan [4] presented the effects of material in-homogeneity on the stress response for the linearly isotropic solid disc or cylinder, which was rotated at constant angular velocity. The special case of a body was taken into consideration with Young's modulus only depends on radial coordinate with constant Poisson's ratio. It was observed that the stress of in-homogenous disc or cylinder was significantly different from homogenous body.

You *et al.* [5] developed a numerical method for the analysis of stresses and deformations in elastic plastic rotating discs with arbitrary variable thickness and density. Runge Kutta method was used to solve governing equation. The governing equation was derived from the

equilibrium equation by inducing a suitable stress function. The computed results from existing approach were compared with finite element method.

Eraslan and Orcan [6] had investigated elastic plastic deformation of an exponential varying thickness disc by using Tresca's yield criteria. It was observed that the reduction in the thickness with increasing the value of the parameter n, the plastic limit angular velocity found increased. Efficient and economical design could be achieved by permitting elastic plastic deformation and by an appropriate choice of the thickness parameters in the applications.

Callioglu [8] had investigated stress analysis on a glass fiber/epoxy orthotropic rotating hollow disc under thermal loads by using analytical solution. Temperature profile was considered varying parabolically from inner to outer surface along the radial section. It was observed that tangential stress decreases at the inner radius while it increases at the outer radius with increase in temperature. Radial stress decreased when temperature increases from zero and maximum variation was observed in the middle region of the disc. The radial displacement had higher values at the outer surface than at the inner surface.

Callioglu *et al.* [9] investigated elastic plastic stress analysis on orthotropic rotating annular disc by using analytical solution. The disc used for analysis was manufactured from curvilinear steel fibers. These curvilinear steel fibres were embedded in aluminum metal matrix by using compression molding method. A few angular velocities were taken into the consideration for an analysis to see the separation of plastic region. It was observed that at the inner surface of the disc plastic yielding occurs first where the tangential stress was the greatest. Magnitude of the circumferential stresses components was higher than the magnitude of radial stresses components. At the inner surface of the disc, residual stresses were observed higher than that of the outer surface. The radial displacement increased at the inner and outer surfaces of the disc.

Eraslan and Akis [10] obtained closed form solutions for functionally graded rotating solid shaft and rotating solid disc by considering the nonlinear variation of the modulus of elasticity in radial direction. Modulus of elasticity (E), of the rotating shaft assumed varying radially in two forms, one is exponential and other is parabolic. Elastic behaviour of rotating functionally graded material shafts was seen to be similar to that of a homogeneous shaft and a rotating homogeneous solid shaft fails with respect to plastic deformation at the centre.

Witek [11] indicated the critical areas of the turbine disc, from the point of view of stress analysis and analyzed the damage mechanisms of the turbine disc subjected to operational and over speed condition by using finite element model. Fracture was observed at 3^{rd} lower slot of the dovetail rim region of the disc, in the speed range of 14,500 to 16,000 rpm due to excessive stresses. It was noticed that damage of the turbine wheel was possible also at lower speed, when the volume of the disc will contain a preliminary fatigue crack. Middle zone of the disc found critical because the engine casing could be punctured by the larger fragments of the disc.

You *et al.* [13] proposed a closed form solution of rotating functionally graded circular disc subjected to constant angular velocity and a uniform temperature change and power law used to describe the variations of Young's modulus, thermal expansion coefficient and density of rotating disc. The effect of varying material properties, radius ratios, different temperature changes and the variation of each material coefficient on stresses and deformation in rotating disc was examined. Two cases were considered for analysis. Material coefficients such as e_1, α_1 and ρ_1 for second case were considered reverse of those in the first case and other material coefficients were kept constant. It was observed that different combinations of material coefficients influence the stresses and radial displacement in the rotating disc influence strongly. When the material coefficients are changed from the first case to second case the radial stress was observed lower, the circumferential stress was increased at the outer radius but decreased at the inner radius and radial displacement increased through the whole thickness of the disc. The effect of the temperature also observed on the stresses and the displacement in the rotating disc. The circumferential stress was raised at the inner radius but reduced at the outer radius of the disc and radial stress increased slightly but radial displacement increased greatly by increasing the temperature.

Altan *et al.* [14] carried out elastic plastic stress analysis on aluminum composite disc under parabolic temperature distribution by using an analytical solution. The aluminum disc was reinforced by steel fibers and manufactured under hydraulic press. Plastic yielding observed at the inner surface of the composite disc first. Plastic region found expanded from inner to outer radius by increasing temperature. The magnitude of tangential stress components observed higher than that of the radial stress components.

Bayat *et al.* [15] presented elastic solutions for axisymmetric rotating discs made of functionally graded material with variable thickness. Two different thickness profiles namely

parabolic and hyperbolic forms were considered. The effects of the grading index (n) and geometry of the disc based on different thickness profiles on the stresses and the radial displacements were investigated. Numerical results had been presented for the functionally graded disc using aluminum as the inner surface metal and zirconia as the outer surface ceramic. It was observed for same grading index (n), concave thickness profile was the lightest disc followed by linear and convex, whereas uniform thickness gave the heaviest. The radial stress in functionally graded discs found decreased with increase in grading index (n), for each thickness profile. Stresses and displacements found smaller in hollow functionally graded rotating discs with hyperbolic convergent profile as compared to uniform thickness.

Hojjati and Hassani [16] presented stress and strain analysis of rotating discs of variable thickness and density by using theoretical and numerical methods. Runge Kutta (RK) method and finite element (FE) modelling of the disc was used to solve the governing differential equations in the plastic and elastic regions. Both the methods were compared with each other. An approximate method called the variable material properties (VMP) was used to solve cases with no exact solutions. Better agreement was observed between the VMP and FE results than between the RK and other results.

Pankaj [17] analyzed elastic plastic transitional stresses in an isotropic disc under internal pressure by using Seth's transition theory. Disc was made of compressible material and having variable thickness. It was concluded that disc made of incompressible material with variable thickness, yields at a higher pressure as compared to disc made of compressible material. A flat disc made of incompressible material yields at internal surface at higher pressure as compared to disc made of compressible material. Maximum circumferential stress was observed at the outer surface of the variable thickness disc.

Zenkour [18] had considered two composite structures of functionally graded material to analyse stress distribution. Accurate analytical solution was presented for the rotating of such structures subjected to different conditions. The composite structures were composed of three layer sandwich solid discs with faces made of different isotropic materials and core made of functionally graded material. The inner layer of structure-1 was made of a metal material and outer layer was made of ceramic material while the core was metal rich at the first inter surface and ceramic rich at second interface, between these two surfaces material properties vary according to a simple gradation relation. Structure-2 was considered by rearranging the

material properties of metal and ceramic. The exponential variation of Young's modulus and density allowed exact solution for the problem. The stresses and displacement distributions were smooth through the radial direction of the composite discs.

Afsar and Go [19] developed finite element model to analyze the thermo elastic field in a rotating functionally graded material (FGM) circular disc considering the incompatible eigenstrain developed in the disc due to non uniform coefficient of thermal expansion and non uniform temperature distribution. It was found that the thermo elastic field in an FGM disc significantly influenced by the temperature distribution profile, radial thickness, angular speed, inner and outer surface temperature difference. Thus, the thermo elastic field in an FGM disc could be controlled and optimized by controlling these parameters.

Callioglu [20] presented the effect of property gradation, centrifugal body loading, thermal loading, internal and external pressure on stresses and displacement in a functionally graded disc. For this purpose, small deformation of theory of elasticity and for graded parameters power law functions were used in the solution procedure. It had been observed that gradient index (n) play an important role to determine the thermo mechanical response of the functionally graded disc.

Deepak *et al.* [21] had presented creep behaviour in functionally graded rotating disc made of composite containing silicon carbide particles in a matrix of pure aluminium. Disc thickness profile considered was of linearly varying from inner to outer radius and threshold stress based creep law was used to describe the creep behaviour by assuming stress exponent 5. The distribution of SiC_p in the functionally graded material disc decreased linearly from inner to outer radius, therefore, the creep constants and the density also varied with radial distance. It had been observed that the presence of particle gradient in a disc, the tangential stress decreased at the inner radius but increased at the outer radius and radial stress increased everywhere with increase in particle content. Better strain rates were observed in functionally graded rotating disc with linearly decreasing particle contents from inner to the outer radius to that observed in a disc containing uniform distribution of reinforcement.

Rattan *et al.* [22] investigated the creep response of an isotropic functionally graded rotating disc made of aluminum silicon carbide particulate composite by using Sherby's model. The effect of material properties on the distributions of stress and strain through the radial direction of the rotating disc had been investigated. The material parameters of creep was

assumed to vary with radial direction in the rotating disc due to varying composition and this had been estimated by regression fit of the available experimental data. It had been concluded that creep behaviour in a rotating disc could be controlled by using suitable particle contents. Strain rates were found minimum in functionally graded disc with parabolic profile than those with uniform distribution or linear variations of particle.

Callioglu *et al.* [23] carried out stress analysis on functionally graded disc rotating at constant angular velocity subjected to linearly increasing and decreasing temperature and effect of internal pressure was also considered. The material was assumed to be isotropic with constant Poisson's ratio (υ) and Young's modulus of elasticity (E), density (ρ) and thermal expansion coefficient (α) assumed to be varying along radial direction. For this purpose, small deformation of theory of elasticity and for graded parameters power law functions were used in the solution procedure. In this study two discs were considered for the analysis. Disc 1 made of functionally graded material with ceramic rich at inner surface and Disc 2 made of functionally graded material with metal rich at inner surface. Radial as well as tangential stresses were noticed higher in Disc 1 when compared with Disc 2. So, the material properties of Disc 2 recommended in orders carrying more loads. Higher radial displacement values were observed in the both discs when subjected to uniform temperature when compared with linearly increasing and decreasing temperature. In Disc 1, tangential stress increased at the inner surface while it decreases at the outer surface with uniformly increasing temperature. For Disc 2, tangential stress was observed to be decreasing at inner radius but increasing at outer radius with increase in temperature.

EkhteraeiToussi *et al.* [24] analyzed the limiting speed and behavior of the disc by discretization (by considered mathematical model in which structure was decomposed to several fictitious elements) and elastic-plastic imaging method. It was seen that touching the limit speed did not necessarily result in an unlimited level of deformation. However, in Ramberge Osgood material, the increase of rotational speed beyond the limit speed increases the deformation in the disc gradually. It was seen that if the thickness profile of the disc is uniform (i.e., constant thickness disc) the quantity of thickness did not affect the limit speed.

Loghman *et al.* [25] presented time dependent creep stress redistribution analysis of $Al-SiC$ rotating disc by using Mendelson's method of successive elastic solution. Radial dependent properties such as elastic modulus, thermal conductivity and coefficient of heat expansion were based on volume fraction percent of SiC reinforcement. The material creep

behavior was described by Sherby's constitutive model. It was concluded that uniform reinforcement did not considerably influence on stresses. It had been found that the stresses, displacement and creep strains were changing with time at a decreasing rate so that after almost 50 years the solution approaches the steady-state condition.

Kansal and Parvez [27] had carried out the thermal stress analysis of orthotropic graded rotating annular disc rotating at constant velocity by using infinitesimal theory of elasticity and for functionally graded case power law function was used. Temperature was varying parabolically from inner to outer surface. Thermal expansion coefficient found decreased when elasticity modulus and density increased. At the inner surface the tangential stress components were found highest but lowest at the outer surface for both discs. When the temperature was increased the radial stress components found decreased gradually along the radial direction.

Sharma *et al.* [29] presented stress and strain analysis of a rotating functionally graded material thermo elastic disc by using finite element method (FEM). They concluded that for fixed angular velocity the stress, strain and displacement of functionally graded circular disc get significantly modified due to uniform temperature variation, logarithmic thermal changes and non-heat conducting (isentropic) conditions. It was concluded that the thermo elastic field in functionally graded material disc could be modeled and optimized by controlling thermal variations, radial thickness and temperature difference at inner and outer surfaces of the disc.

Garg *et al.* [30] analyzed the steady state creep in a rotating functionally graded disc in the presence of linear thermal gradient by using threshold stress based creep law. Linearly varying thickness profile of the rotating disc was considered and disc was made of composite containing silicon carbide particles in a matrix of pure aluminium. The contents of silicon carbide particles were considered decreasing from inner to outer radius in the rotating disc. When the functionally graded disc operated under a linear thermal gradient, the tangential stress increased near the inner radius but decreased towards the outer radius and radial stress was noticed increasing at the entire radius. Strain rates found decreased significantly in the presence of thermal gradient.

Shahzamanian *et al.* [31] had presented elastic contact analysis of functionally graded brake disc by using finite element analysis (FEA). The disc had uniform thickness and subjected to

centrifugal body force, thermal loads, bending loads and friction due to contact condition was considered. The material properties of the brake disc were assumed to be represented by a power law distribution along the thickness, where the free surface was full-metal and contact surface was full-ceramic. The effects of grading index (n) on the displacement, contact status, strain and stress were investigated. It had been concluded that grading index (n) is an important criteria for the design of functionally graded brake discs for automotive and aircraft applications.

2.1 LITERATURE SUMMARY

After carrying out extensive literature survey, it can be concluded that a lot of work has been carried out numerically on FGMs. Nevertheless, the mechanical and mathematical modelling is currently an active research area.

Many researchers Shukla [3], Singh and Ray [7], Deepak *et al.* [21], Ratan *et al.* [22], Loghman *et al.* [25] and Garg *et al.* [30], conducted the study on functionally graded rotating disc were related to creep analysis. Reddy *et al*. [1] and Guven [2] presented a closed form solution for stresses and radial displacement in a rotating disc with varying thickness and density. Horgan and Chan [4] studied the stress response of FGM disc. You *et al.* [5] developed a numerical method for the analysis of deformations and stresses in elastic-plastic rotating discs. Eraslan *et al.* [6] presented elastic plastic deformation of linear hardening rotating disc with variable thickness in an exponentially form. Witek [11] presented the failure analysis of turbine disc of an aerospace engine. You *et al.* [13] analyzed the effect of varying material property on rotating circular disc. Altan *et al.* [14] carried out elastic-plastic thermal stress analysis on an orthotropic aluminium metal matrix composite disc. Bayat *et al.* [15] presented elastic solutions for FGM disc by considering parabolic and hyperbolic thickness profiles. Pankaj [17] and EkhteraeiToussi [24] presented elastic plastic stresses and deformation analysis. Zenkour [18] considered two composite structures of functionally graded material solid discs to present the results for displacement and stresses. Callioglu *et al.* [23], Callioglu [20 and 8] and Kansal [27] studied effect of temperature, grading index (*n*), internal and external pressure on stresses and displacement in FGM disc and Sharma *et al.* [29] used finite element method for stress and strain analysis.

2.2 GAPS IN LITERATURE

After going through the literature available on the rotating FGM disc, it reveals that study pertaining to stress analysis in FGM disc of constant thickness is available in literature. But a little work has been reported on stress analysis in rotating FGM disc with non-uniform thickness subjected internal pressure and thermal loading.

CHAPTER 3
RESEARCH PROBLEM

3.1 IDENTIFICATION OF PROBLEM

In engineering, rotating discs have been received a widespread attention due their numerous practical applications in rotating machinery such as, flywheels, braking system of automobiles, turbines, compressors, computer disc drives and in many other applications [21, 23 and 15]. In most of these applications discs are operated under elevated temperature and subjected to high stresses due to the high speed of rotation. Aluminum matrix reinforced with silicon carbide particles, whiskers or fibers offers the excellent mechanical properties like high specific strength and stiffness, and high temperature stability [21]. Composite materials are a class of advance material, but fails through a process called delamination [28]. In recent years, functionally graded materials (FGMs) have attracted the interest of many researchers due to varying properties over a changing dimension [21 and 28].

Due to their numerous practical applications in engineering, the analysis of rotating discs is an important issue. Therefore, it is decided that to carry out a study pertaining to stress analysis in rotating FGM disc of linearly varying thickness, operating under thermal loading and internal pressure. The disc under investigation is made of composite containing silicon carbide particles (SiC_p) in a matrix of pure aluminium. The content of SiC_p in the disc decreases linearly from inner to the outer radius.

3.2 OBJECTIVES OF RESEARCH WORK

The objective of the present study is to investigate the influence of particle content and basic factors such as, thickness gradient (k), grading index (n), thermal loading and internal pressure (p_i) on stresses, strain rates and displacement in a functionally graded rotating disc.

3.3 METHODOLOGY

To achieve the above stated objective the work includes the development of

(i) Constitutive equations.

(ii) Obtaining the solution of equilibrium equation of functionally graded rotating disc along with constitutive equations.

(iii) Development of software code for determining of tangential stress, radial stress, tangential strain rate, radial strain rate and radial displacement distribution in the rotating FGM disc.

(iv) Validation of analytical model with the available numerical results.

(v) Analysis of the results to draw appropriate conclusions.

CHAPTER 4
MATHEMATICAL FORMULATION

In this chapter, a mathematical analysis is carried out to describe the behaviour of stresses, strain rates and displacement in FGM disc of non-uniform thickness rotating at constant angular velocity and subjected internal pressure and various temperature distributions by using infinitesimal deformation theory of elasticity. Young's modulus of elasticity (E), density (ρ) and thermal expansion coefficient (α), are varying through the radial direction. For this purpose, power law function is used. The model has been used for analysis having following thickness and temperature profiles

(i) Linearly varying thickness and

(ii) Parabolically varying temperature

The volume of the entire disc has been kept equal. The material of the disc is assumed to be isotropic with constant Poisson's ratio (υ).

4.1 DISC PROFILE

In this study, the stress analysis has been reported for rotating disc made of functionally graded material (FGM) having *linearly* varying thickness. The inner radius (a) and outer radius (b) of the disc is assumed, respectively, as 200 mm and 500 mm while the average thickness (t) is taken as 5 mm [23]. Disc is assumed rotating at constant angular velocity. The thickness profile (h), of the disc is assumed to vary along radius [17], according to the following form

$$h(r) = h_b \left(\frac{r}{b}\right)^k \tag{4.1}$$

where h_b, k, and r are disc thickness at $r = b$, thickness gradient and radial distance $(a \leq r \leq b)$, respectively.

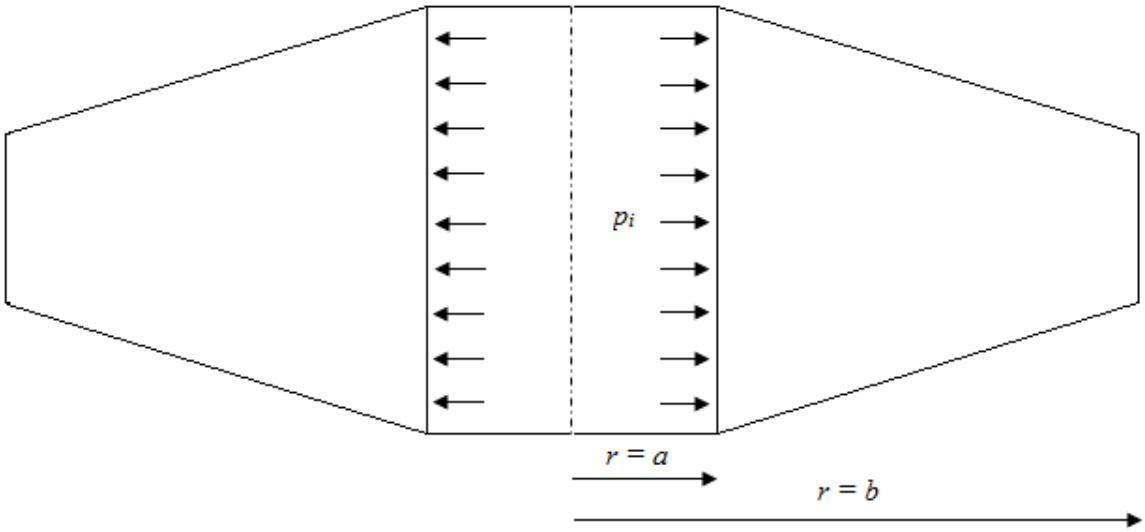

Figure 4.1 FGM disc of non-uniform thickness subjected to internal pressure.

The volume of constant thickness disc is equal to that of linearly varying thickness [21], is given as

$$\int_a^b 2\pi r h(r)\, dr = \pi(b^2 - a^2)t \tag{4.2}$$

Putting the value of $h(r)$ from Eq. (4.1) in Eq. (4.2) and simplifying, one obtains

$$h_b = \frac{(b^2 - a^2)t\ (k+2)b^k}{2\left(b^{k+2} - a^{k+2}\right)} \tag{4.3}$$

4.2 DISTRIBUTION OF MATERIAL PROPERTIES

Material properties of the disc, such as Young's modulus of elasticity (E), density (ρ) and thermal expansion coefficient (α), respectively, are assumed to be varying with *radial distance* [23] and considered as of the following form

$$\begin{cases} E(r) = E\left(\frac{r}{b}\right)^{n_1} \\ \rho(r) = \rho\left(\frac{r}{b}\right)^{n_2} \\ \alpha(r) = \alpha\left(\frac{r}{b}\right)^{n_3} \end{cases} \tag{4.4}$$

where $n_1, n_2,$ and n_3 are grading indexes.

4.3 TEMPERATURE PROFILE

Temperature profile $T(r)$ is considered to change *parabolically* from inner radius to outer radius [8], considered as of the following form

$$T(r) = T_o \times \left(\frac{b^2 - r^2}{b^2 - a^2}\right) \tag{4.5}$$

4.4 DISTRIBUTION OF REINFORCEMENT

The distribution of silicon carbide particles (SiC_p) in FGM disc decreases *linearly* from inner to outer radius [21] of the disc as following

$$V(r) = V_{max} - \frac{(r-a)}{(b-a)}(V_{max} - V_{min}) \tag{4.6}$$

V_{max} and V_{min} are volume content of SiC particles, respectively, at inner (a) and outer (b) radius of the disc. $V(r)$ is volume content of silicon carbide particles (SiC_p), at radius (r).

$$V(r) = A_V - B_V r \tag{4.7}$$

where A_V and B_V terms are

$$A_V = V_{max} + aB_V \tag{4.8}$$

$$B_V = \frac{(V_{max} - V_{min})}{(b-a)} \tag{4.9}$$

Now, using the rule of mixture, the density $\rho(r)$ of the functionally graded disc at any radius (r), may be written as following form

$$\rho(r) = \frac{\rho_{Al}[100 - V(r)] + \rho_{SiC} V(r)}{100} \tag{4.10}$$

$$\rho(r) = \rho_{Al} + \frac{(\rho_{SiC} - \rho_{Al})}{100} V(r) \tag{4.11}$$

Substituting the expression of $V(r)$ from Eq. (4.7) into Eq. (4.11), we get

$$\rho(r) = \rho_{Al} + \frac{(\rho_{SiC} - \rho_{Al})}{100} A_V - \frac{(\rho_{SiC} - \rho_{Al})}{100} B_V r \tag{4.12}$$

$$\rho(r) = A_\rho - B_\rho r \tag{4.13}$$

where ρ_{Al} (= 2700 kg/m^3) and ρ_{SiC} (=3200 kg/m^3) are, respectively, the densities of pure aluminum matrix and silicon carbide particles [25]. Terms A_ρ and B_ρ are given by

$$A_\rho = \rho_{Al} + \frac{(\rho_{SiC} - \rho_{Al})}{100} A_V \tag{4.14}$$

$$B_\rho = \frac{(\rho_{SiC} - \rho_{Al})}{100} B_V \tag{4.15}$$

Similarly, radial dependent property such as modulus of elasticity $E(r)$, can be written as

$$E(r) = A_E - B_E r \tag{4.16}$$

where A_E and B_E terms are given by

$$A_E = E_{Al} + \frac{(E_{SiC} - E_{Al})}{100} A_V \tag{4.17}$$

$$B_E = \frac{(E_{SiC} - E_{Al})}{100} B_V \tag{4.18}$$

where E_{Al} (= 70 GPa) and ρ_{SiC} (= 410 GPa) are, respectively, the modulus of elasticity of pure aluminum matrix and silicon carbide particles [25]. Similarly, thermal expansion coefficient (α) is also obtained.

The average particle content in the disc (V_{avg}) [21] can be expressed as

$$\int_a^b 2\pi h(r)V(r)dr = V_{avg}\pi(b^2 - a^2)t \tag{4.19}$$

$$V_{avg} = \frac{\int_a^b 2\pi h(r)V(r)dr}{\pi(b^2-a^2)t} \tag{4.20}$$

Inserting the expression of $h(r)$ and $V(r)$, respectively, from Eq. (4.1) and Eq. (4.6) into Eq. (4.20) and simplifying, the expression for V_{min} may take the following form

$$V_{min} = \frac{V_{avg} * L - V_{max} * M}{R} \tag{4.21}$$

where $L, M,$ and R terms, respectively, are given below

$$L = (b^2 - a^2)t \tag{4.22}$$

$$M = \frac{2h_b}{b^k(b-a)} \times \left(\frac{b^{k+3} - ab^{k+2}}{k+2} - \frac{ba^{k+2} - a^{k+3}}{k+2} - \frac{b^{k+3}}{k+3} + \frac{a^{k+3}}{k+3} + \frac{ab^{k+2}}{k+2} - \frac{a^{k+3}}{k+2}\right) \tag{4.23}$$

$$R = \frac{2h_b}{b^k(b-a)} \times \left(\frac{b^{k+3}}{k+3} - \frac{a^{k+3}}{k+3} - \frac{ab^{k+2}}{k+2} + \frac{a^{k+3}}{k+2}\right) \tag{4.24}$$

4.5 EQUILIBRIUM EQUATION OF ROTATING DISC

Considering the equilibrium of forces acting on an element of the element of the disc having varying thickness, the force of equilibrium equation [21] may be written as the following form

$$\frac{d}{dr}[h(r)r\sigma_r] - h(r)\sigma_\theta + \rho(r)\omega^2 r^2 h(r) = 0 \tag{4.25}$$

where σ_r, σ_θ, $\rho(r)$, $h(r)$, and ω are, respectively, radial stress, tangential stress, radially varying material mass density, thickness at any radius and angular velocity.

4.6 BOUNDARY CONDITIONS

The boundary conditions for the rotating FGM disc are assumed to be as follow

$$\begin{cases} \sigma_r = -p_i & at\ r = a \\ \sigma_r = 0 & at\ r = b \end{cases} \tag{4.26}$$

4.7 MATHEMATICAL FORMULATION FOR STRESS ANALYSIS

Using the small deformation theory of elasticity, radial displacement (u) [23] can be determined as

$$u = \frac{r}{E(r)}\left(\sigma_\theta - \upsilon\sigma_r\right) + r\alpha(r)T(r) \tag{4.27}$$

The relations between the radial displacement (u) and the strains are irrespective of thickness and the density of the rotating disc [23] can be written as

$$\varepsilon_\theta = \frac{u}{r} \quad or \quad u = \varepsilon_\theta r \tag{4.28}$$

$$\varepsilon_r = \frac{du}{dr} \tag{4.29}$$

Putting the value of u from Eqn. (4.28) into Eq. (4.29), a simple compatibility equation may be written as following form

$$\varepsilon_r = \varepsilon_\theta + r\frac{d\varepsilon_\theta}{dr} \tag{4.30}$$

where $\varepsilon_r, \varepsilon_\theta,$ and u are, respectively, the radial strain, tangential strain and displacement in the radial direction.

The deformation of the disc consists of elastic and plastic components. For the elastic formation, the relations between stresses and strains can be described with using Hook's Law for plane stress case [23] in the following form

$$\varepsilon_r = \frac{1}{E(r)}(\sigma_r - \upsilon\sigma_\theta) + \alpha(r)T(r) \tag{4.31}$$

$$\varepsilon_\theta = \frac{1}{E(r)}(\sigma_\theta - \upsilon\sigma_r) + \alpha(r)T(r) \tag{4.32}$$

where υ is Poisson's ratio which is taken as constant i.e. $\upsilon = 0.3$.

The equation of equilibrium (4.25) is satisfy by the stress function F [9] defined by given form

$$\sigma_r = \frac{F}{rh(r)} \tag{4.33}$$

Using Eq. (4.33) in the Eq. (4.25), one obtains

$$\sigma_\theta = \frac{1}{h(r)}\frac{dF}{dr} + \rho(r)\omega^2 r^2 \tag{4.34}$$

Substituting the value of σ_r and σ_θ from Eq. (4.33) and Eq. (4.34) into Eq. (4.31), respectively, one obtains

$$\varepsilon_r = \frac{1}{E(r)}\left[\frac{F}{rh(r)} - \upsilon\left(\frac{1}{h(r)}\frac{dF}{dr} + \rho(r)\omega^2 r^2\right)\right] + \alpha(r)T(r) \tag{4.35}$$

Putting σ_r and σ_θ from Eq. (4.33) and Eq. (4.34) into Eq. (4.32), respectively, we get

$$\varepsilon_\theta = \frac{1}{E(r)}\left[\frac{1}{h(r)}\frac{dF}{dr} + \rho(r)\omega^2 r^2 - \upsilon\left(\frac{F}{rh(r)}\right)\right] + \alpha(r)T(r) \tag{4.36}$$

Inserting ε_r and ε_θ from Eq. (4.35) and Eq. (4.36) into compatibility equation Eq. (4.30), respectively, and simplifying, we get

$$r^2F'' + rF'\left(1 - r\frac{h'(r)}{h(r)} - r\frac{E'(r)}{E(r)}\right) + F\left(\upsilon r\frac{h'(r)}{h(r)} + \upsilon r\frac{E'(r)}{E(r)} - 1\right) = -\rho(r)h(r)\omega^2 r^3\left(\upsilon + 3 - r\frac{E'(r)}{E(r)}\right) - \rho'(r)h(r)\omega^2 r^4 - \alpha'(r)T(r)h(r)\,r^2\,E(r) - \alpha(r)T'(r)h(r)\,r^2\,E(r) \tag{4.37}$$

where

$$F^{"} = \frac{d^2F}{dr^2} \ , \ \ F^{'} = \frac{dF}{dr} \ , \quad h^{'}(r) = \frac{dh}{dr} \ , \quad \rho^{'} = \frac{d\rho}{dr} \tag{4.38}$$

Substitution of Elastic modulus $E(r)$, density $\rho(r)$, coefficient of thermal expansion $\alpha(r)$ from Eq. (4.4), thickness profile from Eq. (4.1) and temperature profile from Eq. (4.5) into second order differential equation (4.37), respectively, and simplifying, we get

$$r^2F^{"} + rF^{'}\left(1 - k - n_1\right) + F\left(vk + vn_1 - 1\right) = -\frac{\rho\,\omega^2\,h_b\,r^{n_2+k+3}}{b^{n_2+k}}\left(v + 3 - n_1 + n_2\right) - \frac{E\,h_b\,n_3\,\alpha}{b^{n_1+n_3+k-2}}\left(\frac{T_o}{b^2-a^2}\right)r^{n_1+n_3+k+1} + \frac{E\,h_b\,\alpha\,(n_3+2)}{b^{n_1+n_3+k}}\left(\frac{T_o}{b^2-a^2}\right)r^{n_1+n_3+k+3} \tag{4.39}$$

where $n_1,\ n_2,\ n_3,$ and k terms, respectively, are

$$n_1 = r\frac{E^{'}(r)}{E(r)},\ n_2 = r\frac{\rho^{'}(r)}{\rho(r)},\ n_3 = r\frac{\alpha^{'}(r)}{\alpha(r)}\ and\ k = r\frac{h^{'}(r)}{h(r)} \tag{4.40}$$

Simplifying Eq. (4.39), the stress function F, take the following form

$$F = C_1\,r^{\frac{k+n_1+m}{2}} + C_2\,r^{\frac{k+n_1-m}{2}} + A\,r^{n_2+k+3} + B\,r^{n_1+n_3+k+1} + C\,r^{n_1+n_3+k+3} \tag{4.41}$$

where C_1 and C_2 are the integration constants. A, B, C and m terms, respectively, are given below

$$A = -\frac{\rho\,\omega^2\,h_b(v+3-n_1+n_2)}{b^{n_2+k}\,(n_2^2 + n_2k + 3k + 6\,n_2 - n_1n_2 - n_1k - 3n_1 + vk + vn_1 + 8)} \tag{4.42}$$

$$B = -\frac{E\,h_b\,n_3\,\alpha}{b^{n_1+n_3+k-2}\left(n_3^2 + n_1n_3 + n_3k + k + n_1 + 2n_3 + vk + vn_1\right)} \times \left(\frac{T_o}{b^2-a^2}\right) \tag{4.43}$$

$$C = \frac{E\,h_b\,\alpha(n_3+2)}{b^{n_1+n_3+k}\left(n_3^2 + n_1n_3 + n_3k + 3k + 3n_1 + 6n_3 + vk + vn_1 + 8\right)} \times \left(\frac{T_o}{b^2-a^2}\right) \tag{4.44}$$

$$m = \sqrt{(-k-n_1)^2 - 4vk - 4vn_1 + 4} \tag{4.45}$$

Now, using the stress function F from Eq. (4.41) into Eq. (4.33) and Eq. (4.34) and simplifying, σ_r and σ_θ may be written as

$$\sigma_r = \frac{C_1\, r^{\frac{k+n_1+m-2}{2}} + C_2\, r^{\frac{k+n_1-m-2}{2}} + A\, r^{n_2+k+2} + B\, r^{n_1+n_3+k} + C\, r^{n_1+n_3+k+2}}{h(r)} \tag{4.46}$$

$$\sigma_\theta = \frac{1}{h(r)}\left(\frac{k+n_1+m}{2}\, C_1 r^{\frac{k+n_1+m-2}{2}} + \frac{k+n_1-m}{2}\, C_2 r^{\frac{k+n_1-m-2}{2}} + (n_2+k+3)\, A r^{n_2+k+2} + (n_1+n_3+k+1)\, B r^{n_1+n_3+k} + (n_1+n_3+k+3)\, C r^{n_1+n_3+k+2}\right) + \rho(r)\omega^2 r^2 \tag{4.47}$$

Substitution of boundary conditions from Eq. (4.26) into Eq. (4.46), give the integration constants C_1 and C_2, which may be, respectively, written as

$$C_1 = \frac{D_2\, b^{\frac{-k-n_1+m+2}{2}} - D_1\, a^{\frac{-k-n_1+m+2}{2}}}{b^m - a^m} \tag{4.48}$$

$$C_2 = \frac{D_1\, b^m\, a^{\frac{-k-n_1+m+2}{2}} - D_2\, a^m\, b^{\frac{-k-n_1+m+2}{2}}}{b^m - a^m} \tag{4.49}$$

where D_1 and D_2 terms , respectively, are as follow

$$D_1 = -p_i\, h(a) - A\, a^{n_2+k+2} - B\, a^{n_1+n_3+k} - C\, a^{n_1+n_3+k+2} \tag{4.50}$$

$$D_2 = -A\, b^{n_2+k+2} - B\, b^{n_1+n_3+k} - C\, b^{n_1+n_3+k+2} \tag{4.51}$$

CHAPTER 5
VALIDATION

It is necessary to check the correctness of analysis and the developed code for calculation of results before actually doing so. For this purpose, the stresses and displacement have been computed in a rotating disc made of functionally graded material (FGM) and have been compared with the available results Callioglu *et al*. [23]. The dimensions, material properties and operating conditions for the FGM disc are summarized in Table 2 of the *Appendix*.

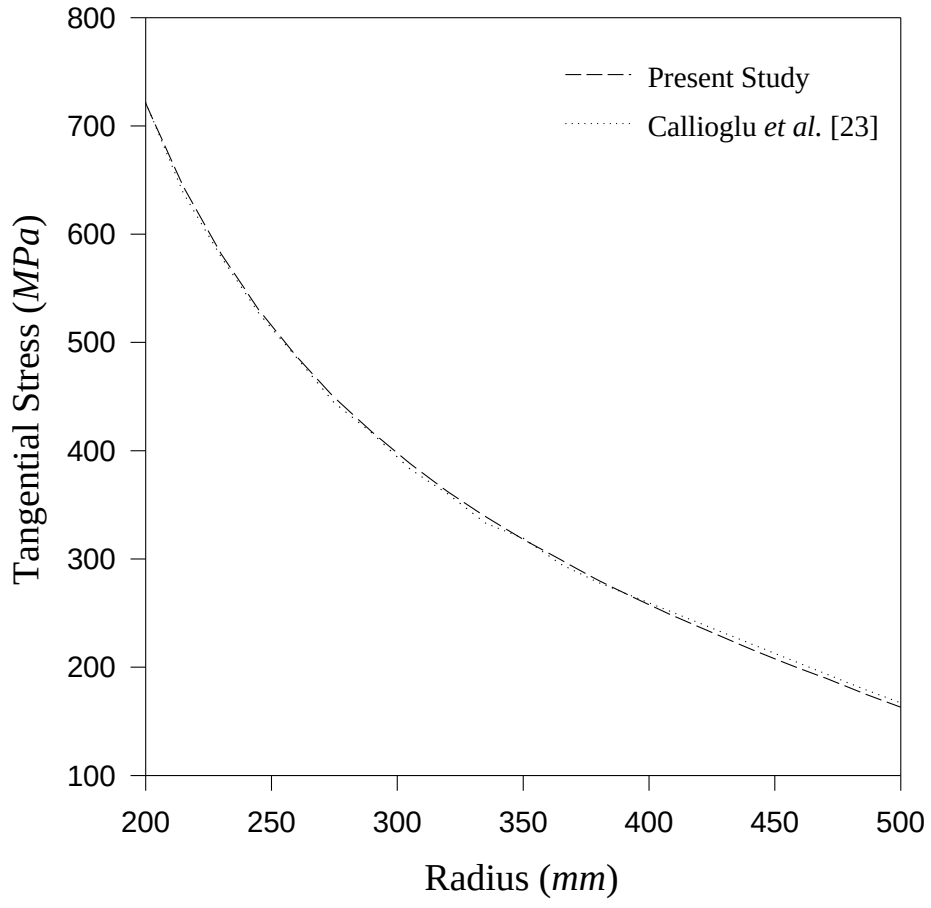

Figure 5.1 Comparison of tangential stress (present study) with published results [23].

The variation of tangential stress along the radius has been showed in Figure 5.1 and the values of radial displacement are given in Table 5.1, which show a good agreement between the two i.e. the results obtained from the present analysis and the published results. So, this validates the present analysis.

Table 5.1: Comparison of the radial displacement values (present study) with published results [23]

Radius (mm)	Displacement (mm)	
	Callioglu *et al.*[23]	Present Study
200	0.583	0.597
250	0.562	0.566
300	0.520	0.560
350	0.541	0.560
400	0.541	0.560
450	0.541	0.555
500	0.533	0.545

CHAPTER 6

RESULTS AND DISCUSSIONS

The aim of the present research work is to investigate the effect of reinforcement and basic factors such as, thickness gradient (k), grading index (n), thermal loading and internal pressure (p_i). In this section, following is the detailed discussion of the obtained results.

6.1 EFFECT OF REINFORCEMENT

The effect of variation in reinforcement at different radii in the rotating disc is observed by keeping total volume fraction of reinforcement same in all the three discs, considered for this purpose. To check the response of stresses, strain rates and displacement, three discs have been considered which are:

(i) **Disc-1** (Non-FGM) having uniform particle distribution of **20 vol. %** throughout
(ii) **Disc-2** (FGM) with maximum particle content of **25 vol. %** and
(iii) **Disc-3** (FGM) with maximum particle content of **30 vol. %.**

The average volume is kept as **20%.**

Regression analysis is carried out to obtain material parameters using data fit analysis. The material properties, operating conditions, grading indexes, dimensions and other parameters of rotating discs are reported in Tables (2)-(5) of the *Appendix*.

The variation of tangential stress along radius is shown in Figure 6.1. By increasing the particle content in FGM discs (Disc-2 and Disc-3) the tangential stress near the inner radius increases but decreases towards the outer radius when compared with variation in tangential stress in Disc-1. The maximum difference in the magnitude of tangential stress corresponding to Disc-3 and Disc-1 is observed as 43 MPa at the inner radius and 17.1 MPa, at the outer radius of the discs. Tangential stress remains same at radius around 305 mm in all the three discs.

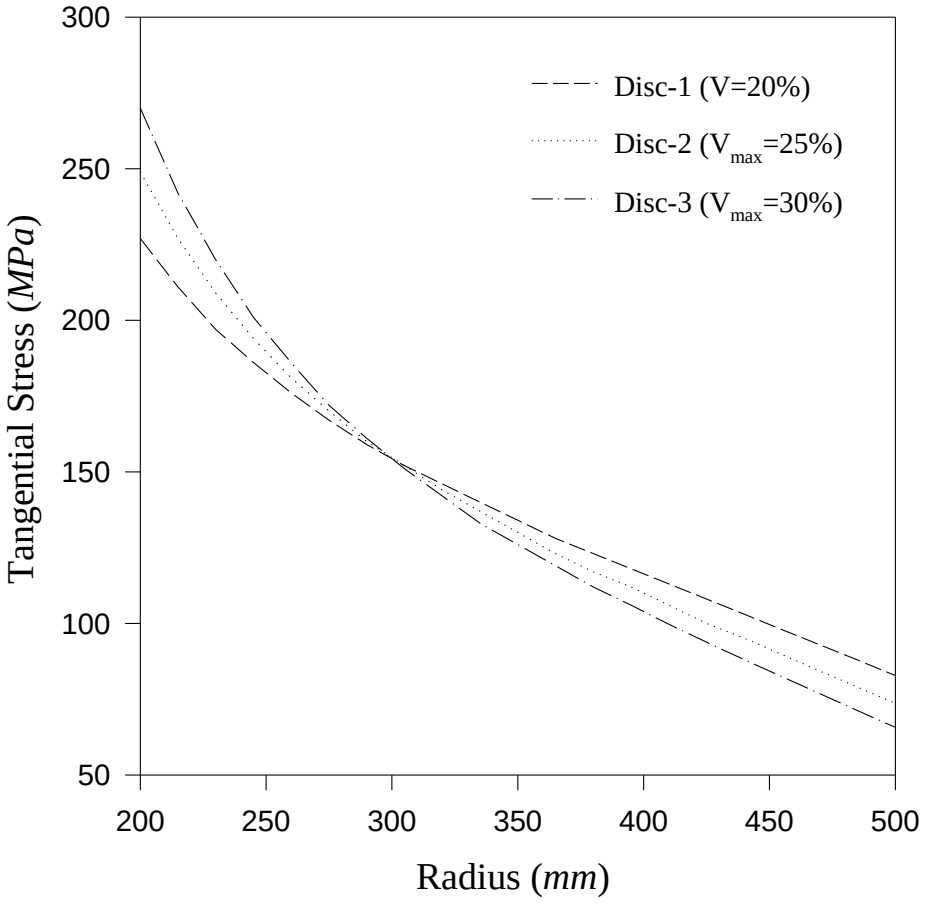

Figure 6.1 Effect of varying particle content on tangential stress.

The radial stress, Figure 6.2, is observed higher in the middle region of FGM discs (Disc-2 and Disc-3) when compared with those observed in Disc-1, having uniform particle distribution. The maximum value of radial stress is observed in Disc-3, which is 47.6 MPa.

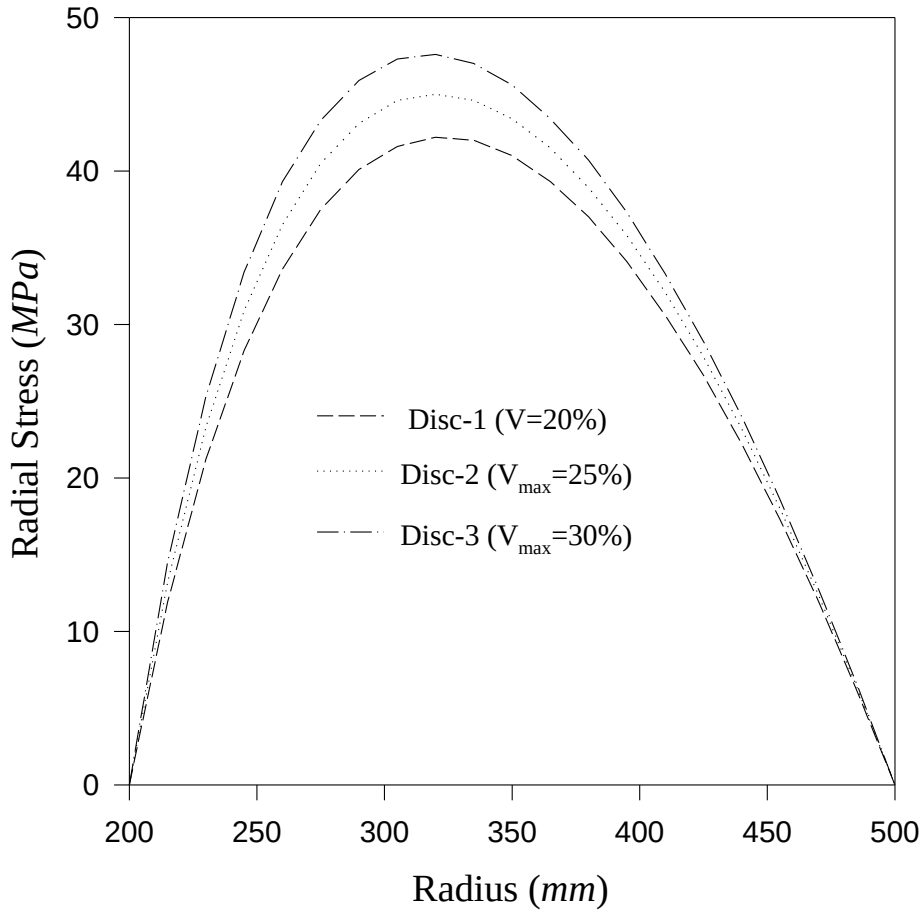

Figure 6.2 Effect of varying particle content on radial stress.

Figure 6.3 illustrates the effect of the particle content on tangential strain rate with radial distance. It can be seen that throughout the disc, the tangential strain rate is maximum for Non-FGM disc (Disc-1) and minimum for FGM disc (Disc-3). The decreasing trend is observed from the inner to outer radius for Disc-1, Disc-2 and Disc-3. In Non-FGM disc, the tangential strain rate changes from 1.65×10^{-3} s^{-1} to 6.00×10^{-4} s^{-1}, respectively, inner to outer radius. In Disc-3, it changes from 1.51×10^{-3} s^{-1} to 5.69×10^{-4} s^{-1}, respectively, inner to outer radius.

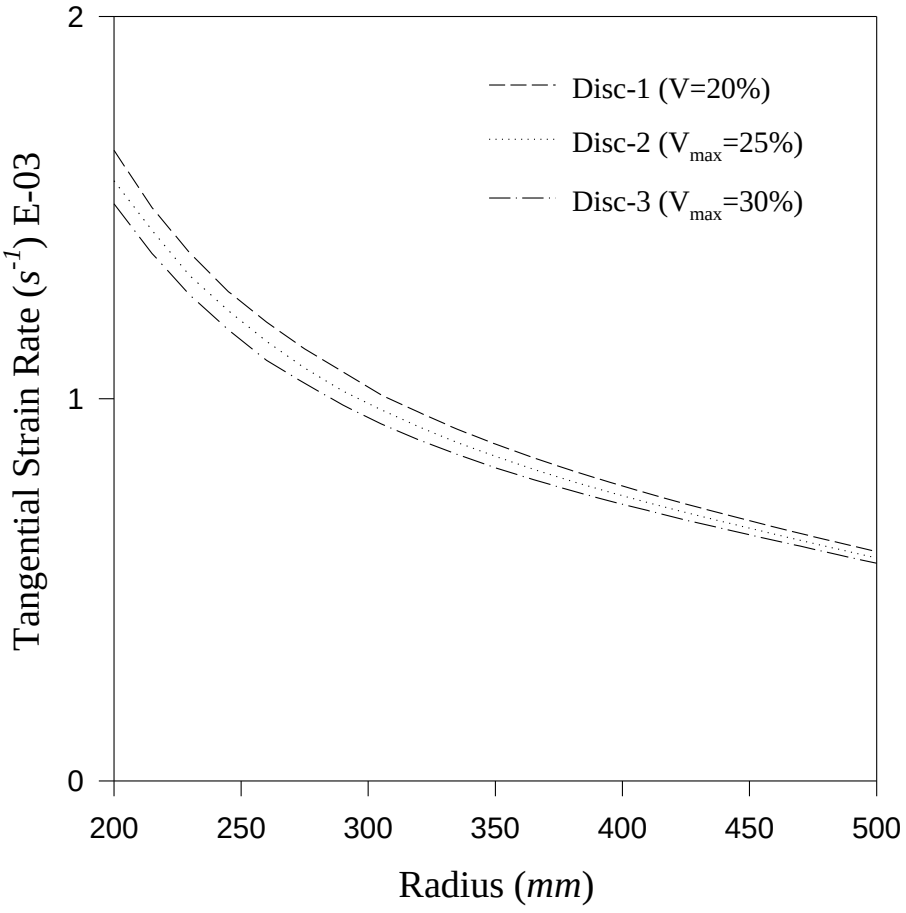

Figure 6.3 Effect of varying particle content on tangential strain rate.

The variation of radial strain rate along the radial distance is shown in Figure 6.4. It can be seen from the figure that the radial strain rate is observed to be compressive near the inner and outer radii of the three discs. At the inner and outer radius, the compressive radial strain rate is observed highest for Disc-1 and lowest for Disc-3. The radial strain rate becomes tensile in the middle region of the three discs.

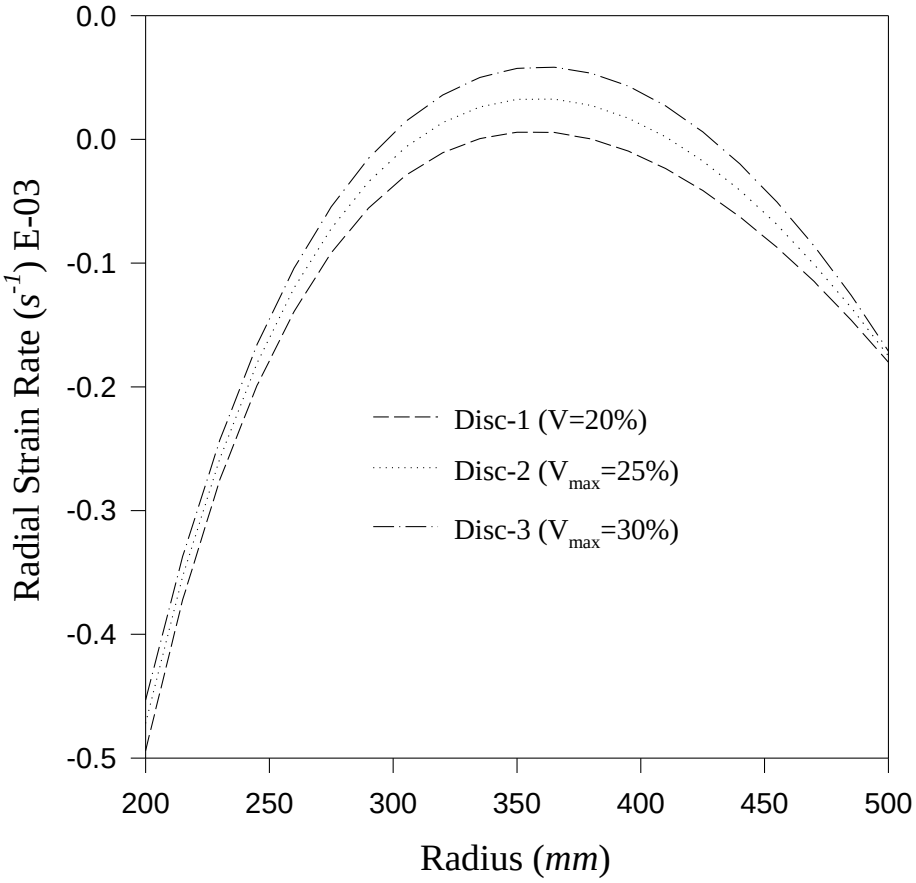

Figure 6.4 Effect of varying particle content on radial strain rate.

Figure 6.5 shows the effect of particle content on radial displacement along the radius. Figure reveals that by increasing the particle content in Disc-2 and Disc-3, the radial displacement decreases over the entire radius as compared to the Disc-1. The maximum variation in radial displacement, corresponding to Disc-1 and Disc-3, is noticed around 0.027 mm and 0.015 mm, respectively, at the inner and outer radius of the discs.

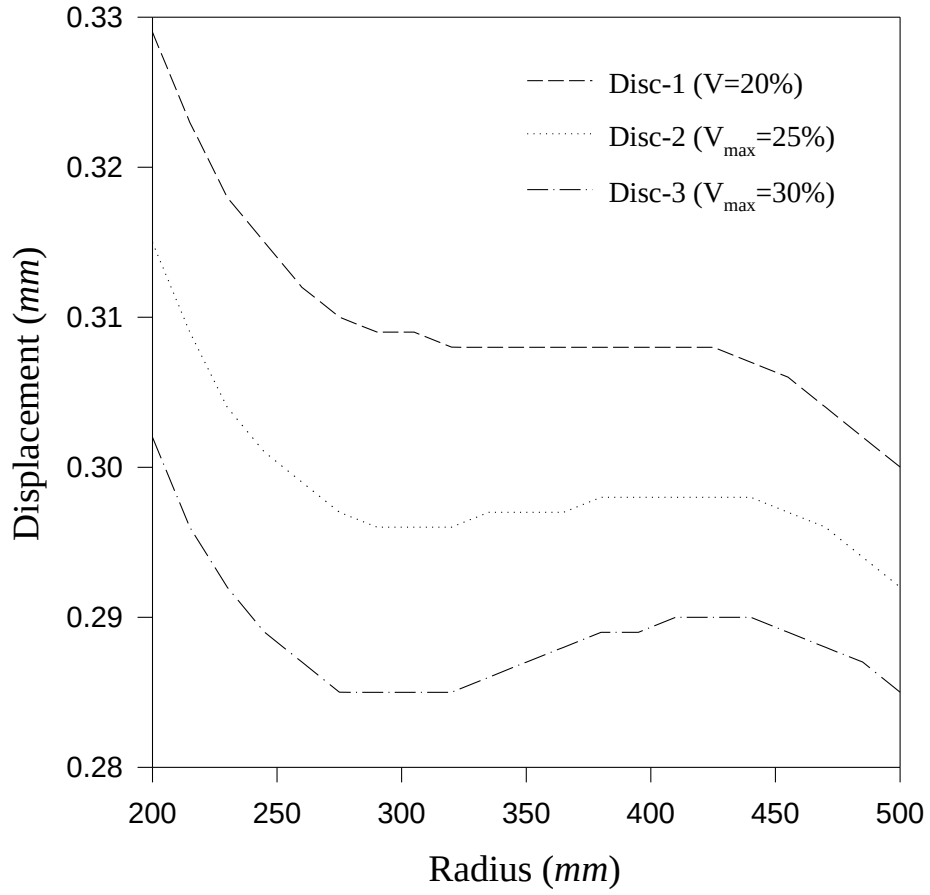

Figure 6.5 Effect of varying particle content on radial displacement.

6.2 EFFECT OF THICKNESS GRADIENT

In this subsection, the effect of the thickness gradient (k) on stresses, strain rates and displacement are presented in Figures (6.6)-(6.10). For this purpose, the required data is reported in Tables (6)-(8) of the *Appendix*. Dimensions of the disc, operating conditions and other parameters are kept same as in the previous section. Three cases are considered to show the effect of thickness gradient:

(i) $\boldsymbol{k}$ **= 0,** represents the **constant thickness** disc and

(ii) $\boldsymbol{k}$ **= -0.2** and **-0.4,** represent the **linearly varying thickness** disc.

Results of non-uniform thickness disc have been compared with constant thickness disc.

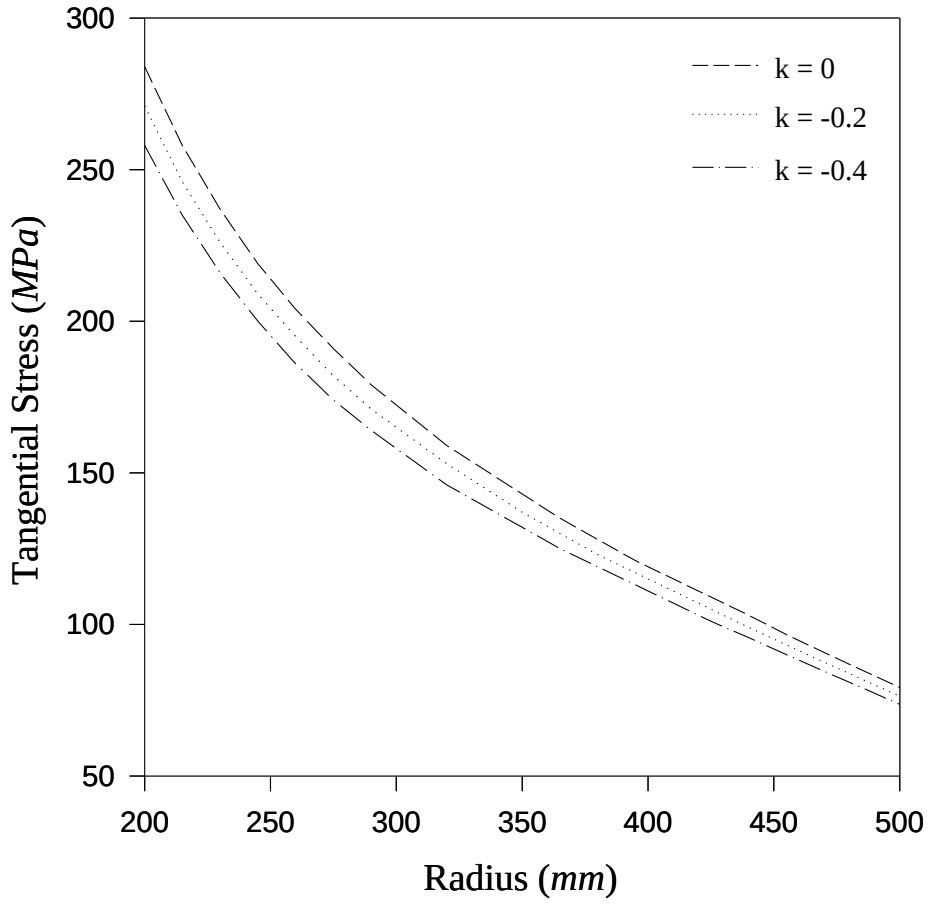

Figure 6.6 Effect of thickness gradient on tangential stress.

The variation of tangential stress along radius is depicted in Figure 6.6. It can be seen from the figure that the tangential stress is maximum in constant thickness disc (k = 0) and minimum for (k = -0.4). The tangential stress decreases gradually throughout the radius. The maximum variation in tangential stress, corresponding to k = 0 and k = -0.4, is noticed around 26 MPa and 5.6 MPa, respectively, at the inner and outer radii of the discs.

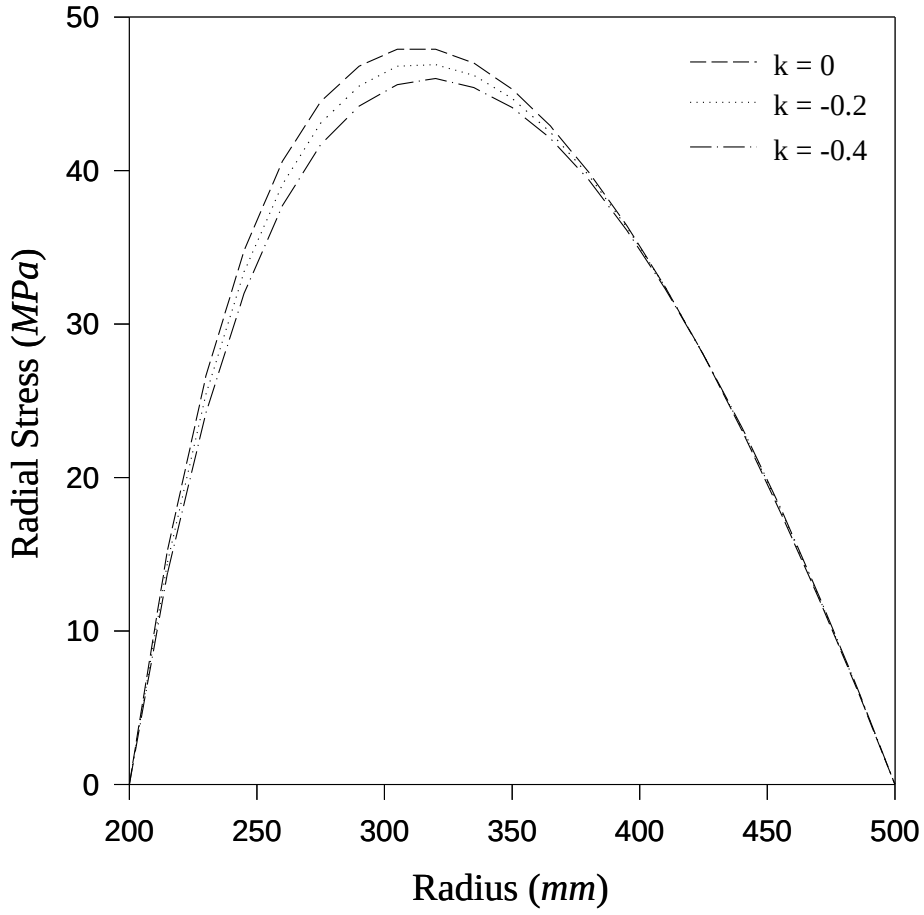

Figure 6.7 Effect of thickness gradient on radial stress.

Figure 6.7 illustrates the variation of radial stress with radial distance. The figure reveals that in the middle region of the disc the radial stress is observed higher in constant thickness disc when compared with those observed in non-uniform thickness discs. The maximum radial stress value is observed as 47.9 MPa at radius 305 mm and 320 mm in constant thickness disc.

The variation of tangential strain rate with radius is shown in Figure 6.8. It can be seen that throughout the radius of the disc, the tangential strain rate is maximum in constant thickness disc and minimum for k = -0.4. In constant thickness disc, the tangential strain rate changes from 1.73×10^{-3} s^{-1} to 6.35×10^{-4} s^{-1}, respectively, inner to outer radius. In non-uniform thickness disc for k = -0.4, the tangential strain rate changes from 1.60×10^{-3} s^{-1} to 5.92×10^{-4} s^{-1}, respectively, inner to outer radius.

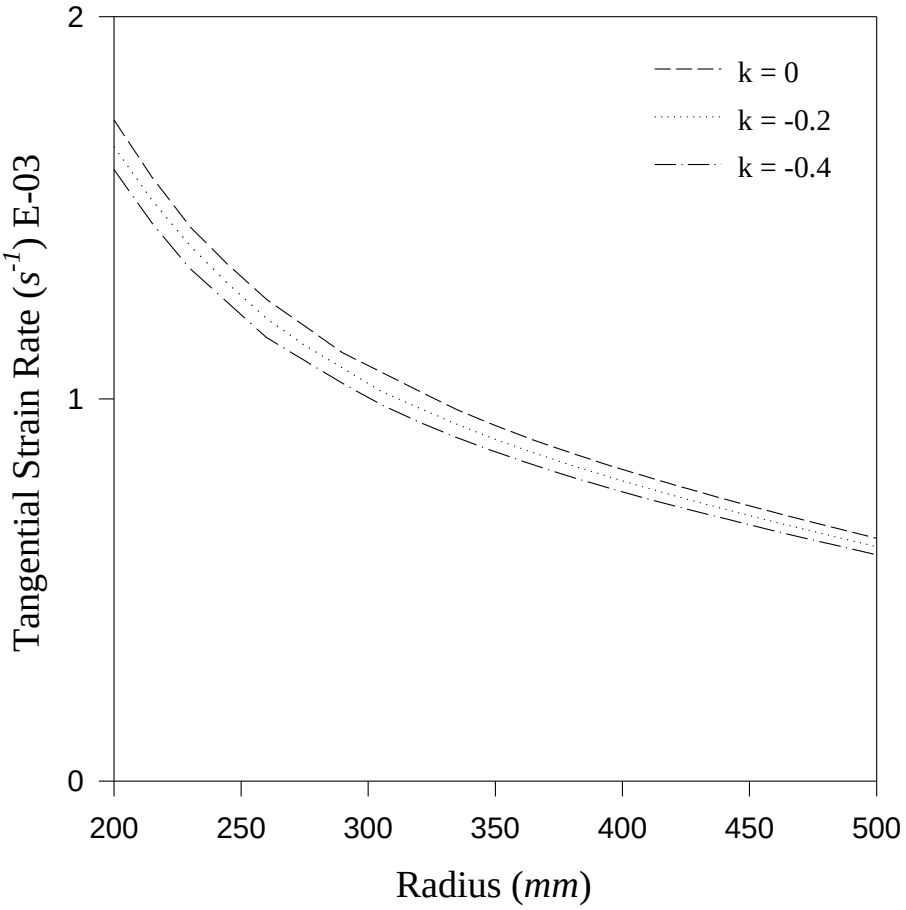

Figure 6.8 Effect of thickness gradient on tangential strain rate.

The radial strain rate, Figure 6.9, is observed to be compressive at the inner and outer radii of the constant thickness disc and varying thickness disc. At the inner and outer radius, the radial strain rate is observed highest for constant thickness disc and lowest for varying thickness disc, having thickness gradient k = -0.4. The radial strain rate becomes tensile in the middle region of the constant thickness disc as well as varying thickness disc.

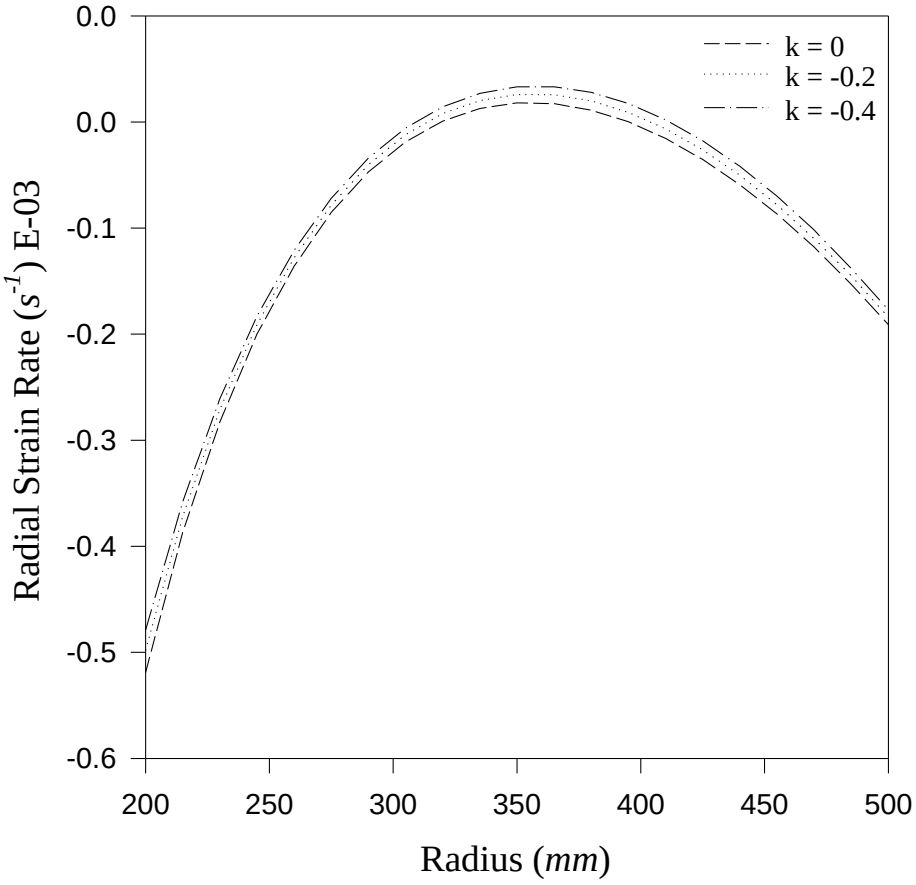

Figure 6.9 Effect of thickness gradient on radial strain rate.

Figure 6.10 shows the variation of radial displacement along the radius. The Figure reveals that in non-uniform thickness disc the radial displacement decreases over the entire radius as compared to constant thickness disc. The maximum variation in radial displacement, corresponding to k = 0 and k = -0.4, is noticed around 0.027 mm and 0.022 mm, respectively, at the inner and outer radius of the disc.

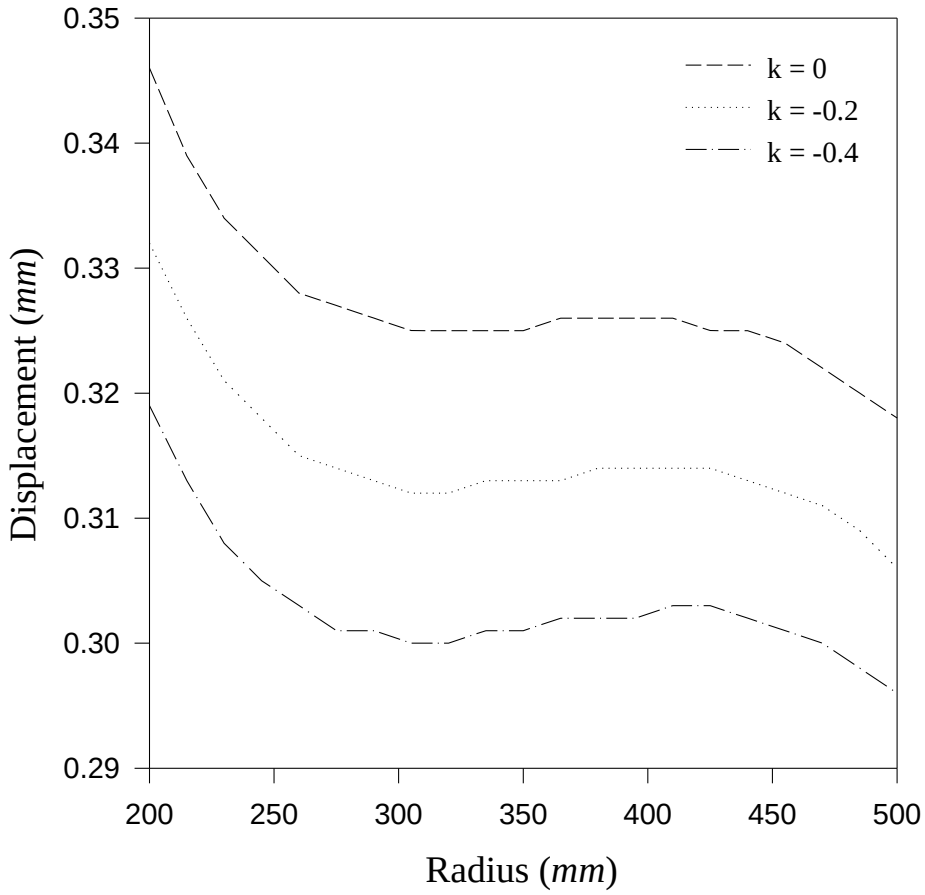

Figure 6.10 Effect of thickness gradient on radial displacement.

6.3 EFFECT OF GRADING INDEX

Grading index (n) is one of the key factors which influence the stresses, strain rates and displacement. Figures (6.11)-(6.15) illustrate the effect of grading index (n) when it varies from 0.5 to -0.5. The material properties such as Young's modulus, density and thermal expansion coefficient of Disc-3, grading index, dimensions and particle content for the disc are summarized in Tables 2, 4 and 5 of the *Appendix*.

The grading index $(n) = n_1 = n_2 = -n_3$ for E, ρ and α, respectively.

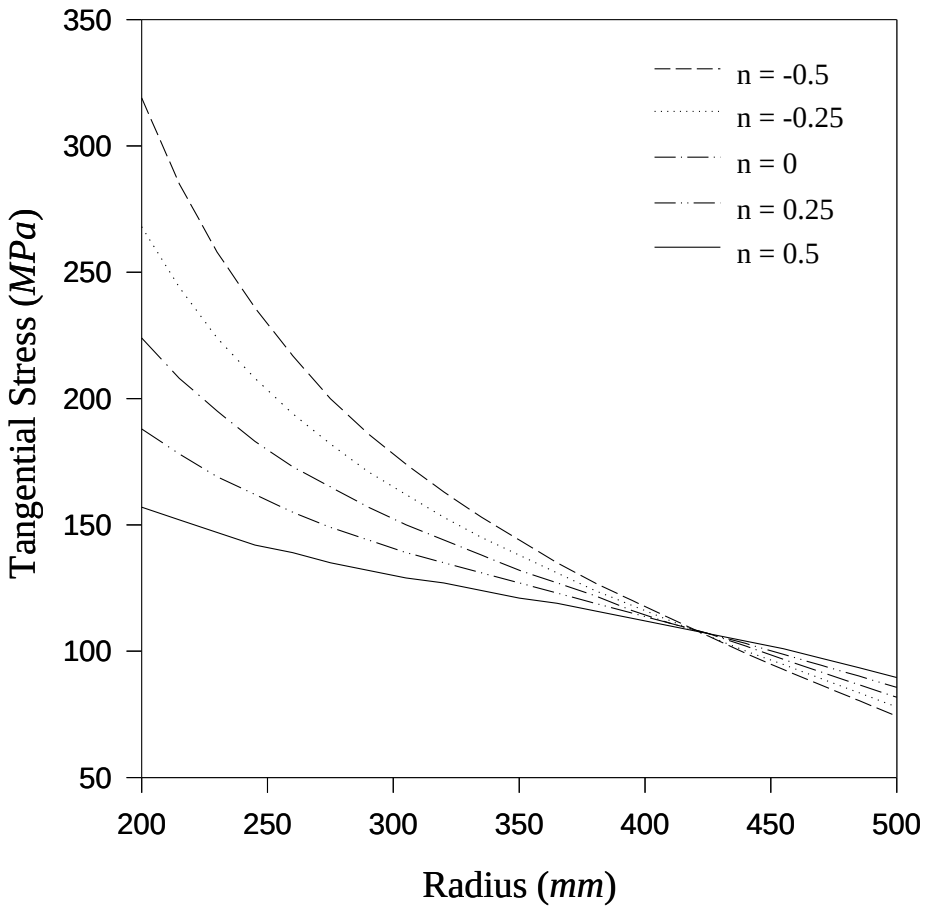

Figure 6.11 Effect of grading index on tangential stress.

The variation of tangential stress along the radial direction is presented in Figure 6.11. At the inner radius of the FGM disc, the tangential stress is relatively higher for n = -0.5 and lower for n = 0.5 and the maximum difference is noticed as 162 MPa. At the outer radius of

the disc, the trend of variation is observed opposite to that observed at the inner radius and maximum difference is observed as 15.3 MPa. Tangential stress remains same at radius around 425 mm for all values of grading index (n).

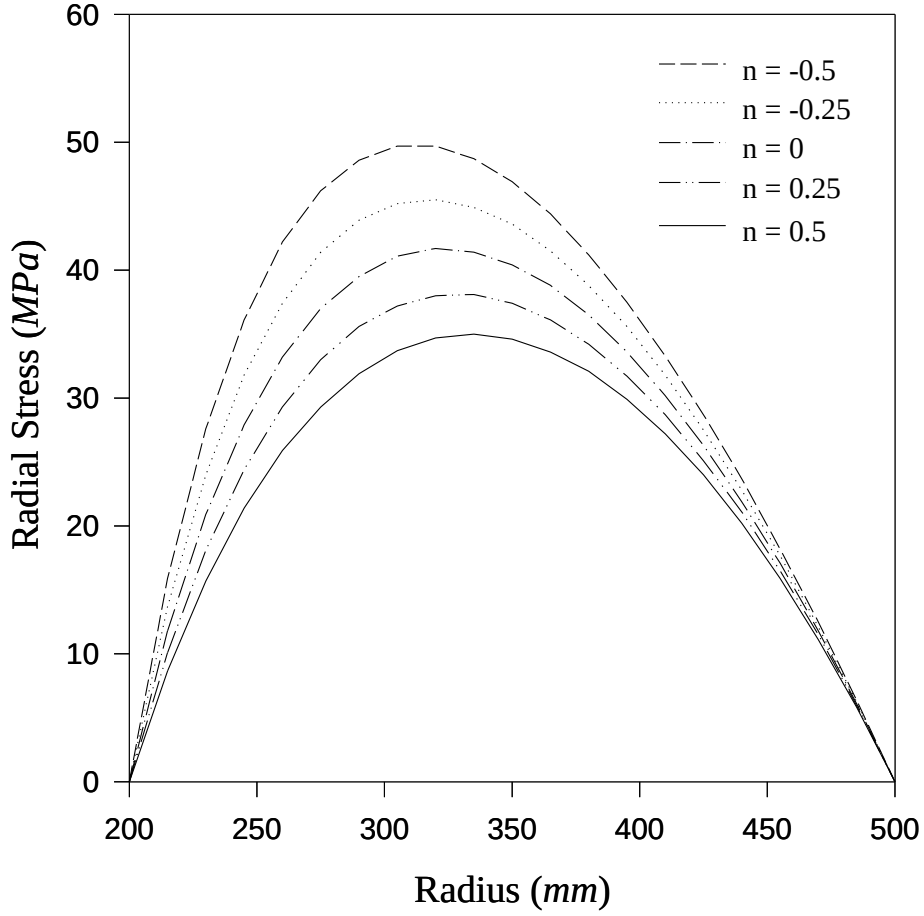

Figure 6.12 Effect of grading index on radial stress.

Figure 6.12 shows the variation of radial stress along radial direction for different values of grading index. The radial stress is observed maximum in the middle region of the FGM disc for grading index (n) = -0.5 and minimum for grading index (n) = 0.5. The maximum value of radial stress value is observed as 49.7 MPa.

The tangential strain rate is significantly affected by varying the grading index, as seen from Figure 6.13. The figure revels that the tangential strain rate is largest for grading index (n) = 0.5 and least for grading index (n) = -0.5 over the entire radius of the disc. For n = -0.5, the tangential strain rate changes from 1.75×10^{-3} s^{-1} to 6.44×10^{-4} s^{-1}, respectively, inner to outer radius. For n = 0.5, it changes from 2.16×10^{-3} s^{-1} to 7.76×10^{-4} s^{-1}, respectively, inner to outer radius.

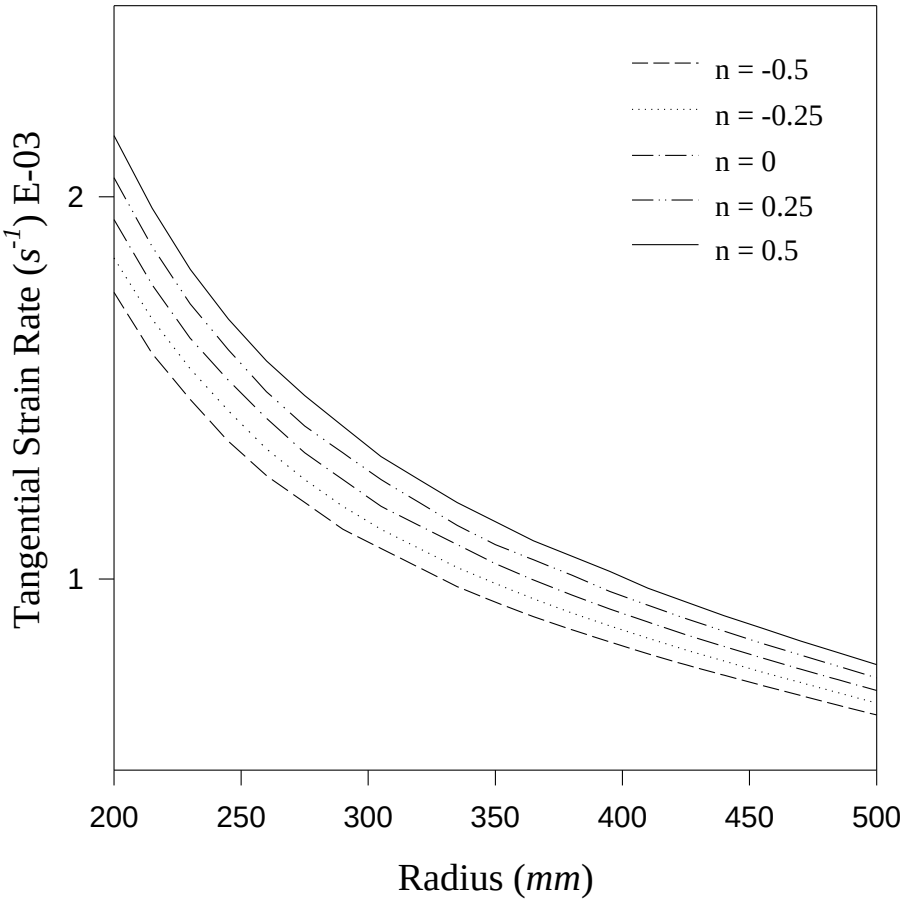

Figure 6.13 Effect of grading index on tangential strain rate.

The variation of radial strain rate along the radius is depicted in Figure 6.14. It can be seen from the figure that the radial strain rate is observed to be compressive at the inner and outer radius of the disc for different values of n. At the inner and outer radii, the radial strain rate is observed highest for n = 0.5 and lowest for n = -0.5. The radial strain rate becomes tensile in the middle region of disc for all the values of n.

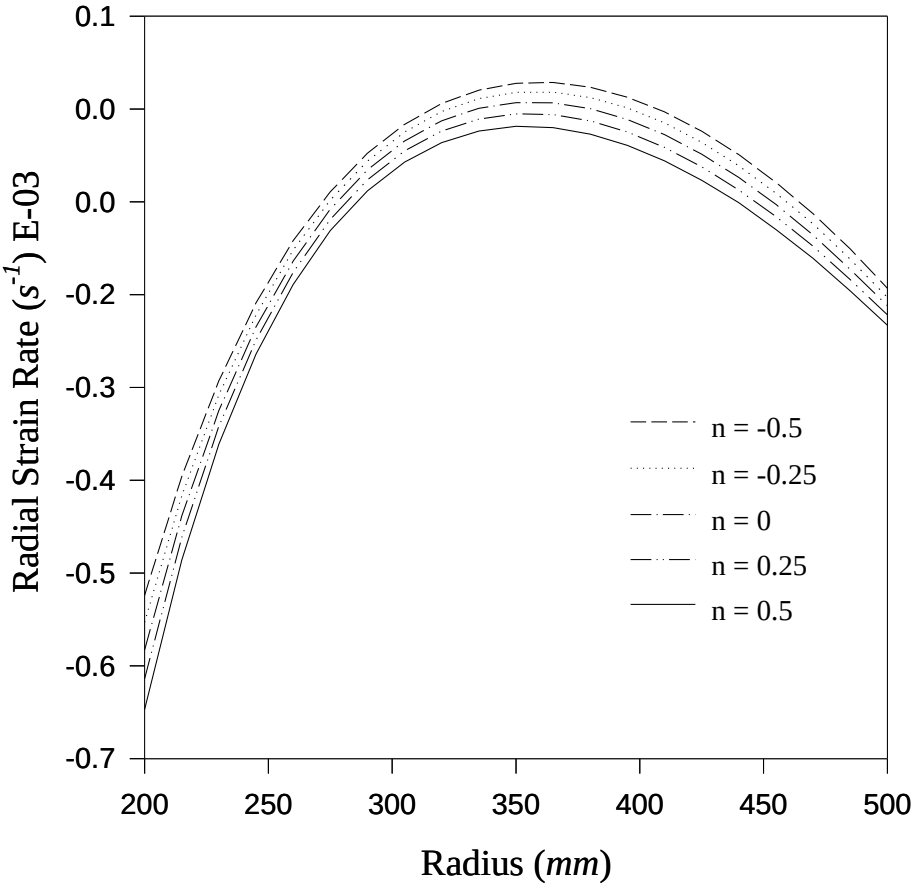

Figure 6.14 Effect of grading index on radial strain rate.

The variation of radial displacement with radius is shown in Figure 6.15. It is observed that the radial displacement is least over the entire radius of the disc for n = -0.5 when compared with other values of n. The maximum variation in radial displacement, corresponding to n = 0.5 and n = -0.5, is noticed around 0.081 mm and 0.066 mm, respectively, at the inner and outer radius of the FGM disc.

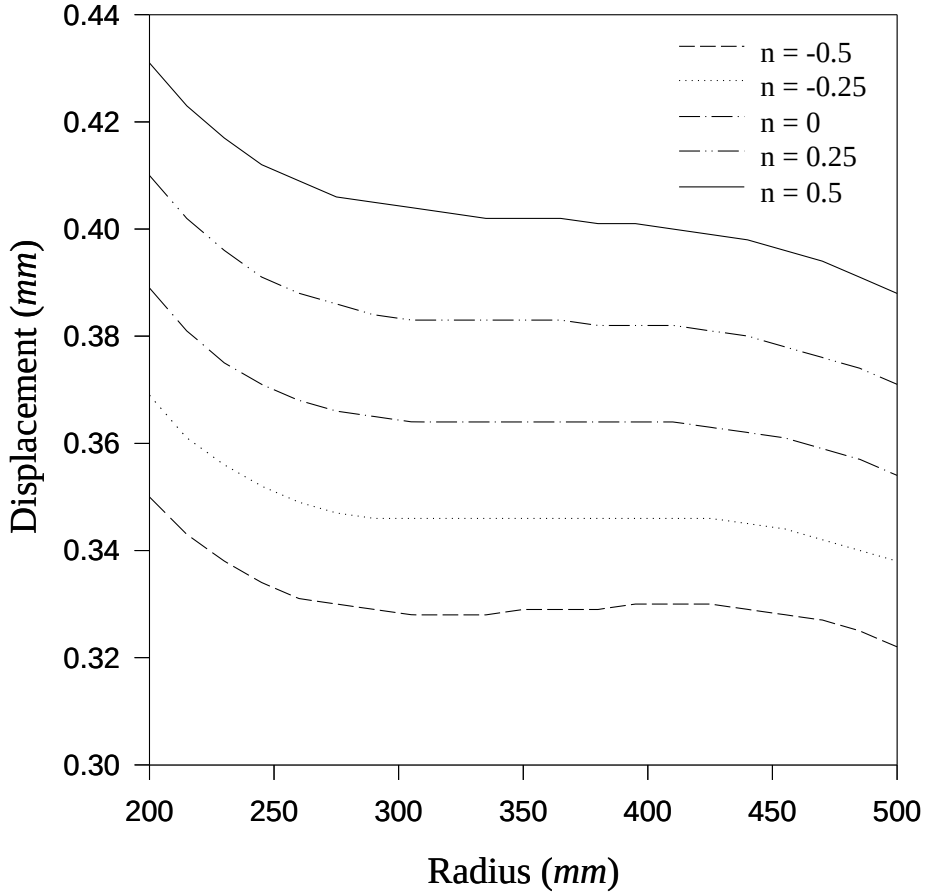

Figure 6.15 Effect of grading index on radial displacement.

6.4 EFFECT OF TEMPERATURE

Figures (6.16)-(6.20) show the effect of temperature on stresses, strain rates and displacement when it varies from 0ºC to 600ºC. For this purpose, the material properties such as Young's modulus, density and thermal expansion coefficient of Disc-3 are considered and reported in Table 2 of the *Appendix*. Grading index (n) and other required data for the FGM disc is summarized, respectively, in Tables (3)-(5) of the *Appendix*.

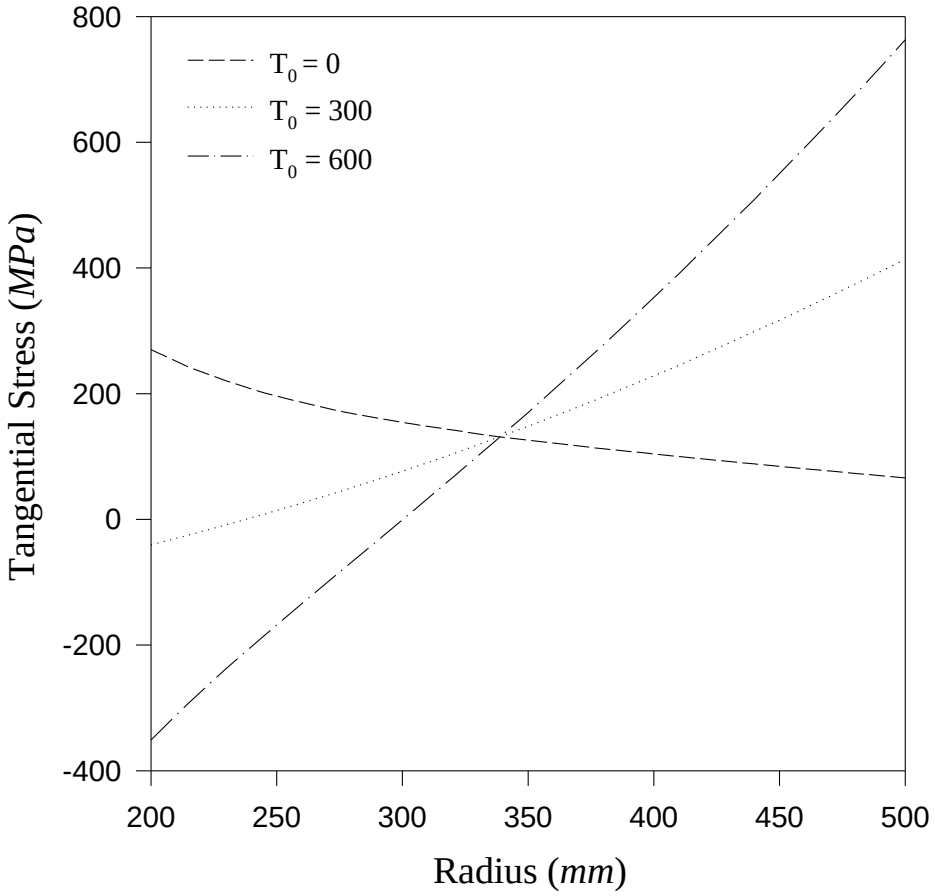

Figure 6.16 Variation of tangential stress along radius with varying temperature.

The effect of temperature on tangential stress with radius is depicted in Figure 6.16. The figure reveals that as the temperature is increased from 0ºC to 600ºC the tensile stress is changing from compressive to tensile as moving from inner radius to outer radius. The maximum difference in the magnitude of tangential stress corresponding to 0ºC and 600ºC is observed as 697.3 MPa at the outer radius of the disc.

The effect of increase in temperature on radial stress can be clearly seen from the Figure 6.17. The radial stress is observed maximum near a radius of 320 mm when the disc is operated at 0ºC. The radial stress is reducing when temperature is increased to 300ºC and became compressive with further increase in temperature.

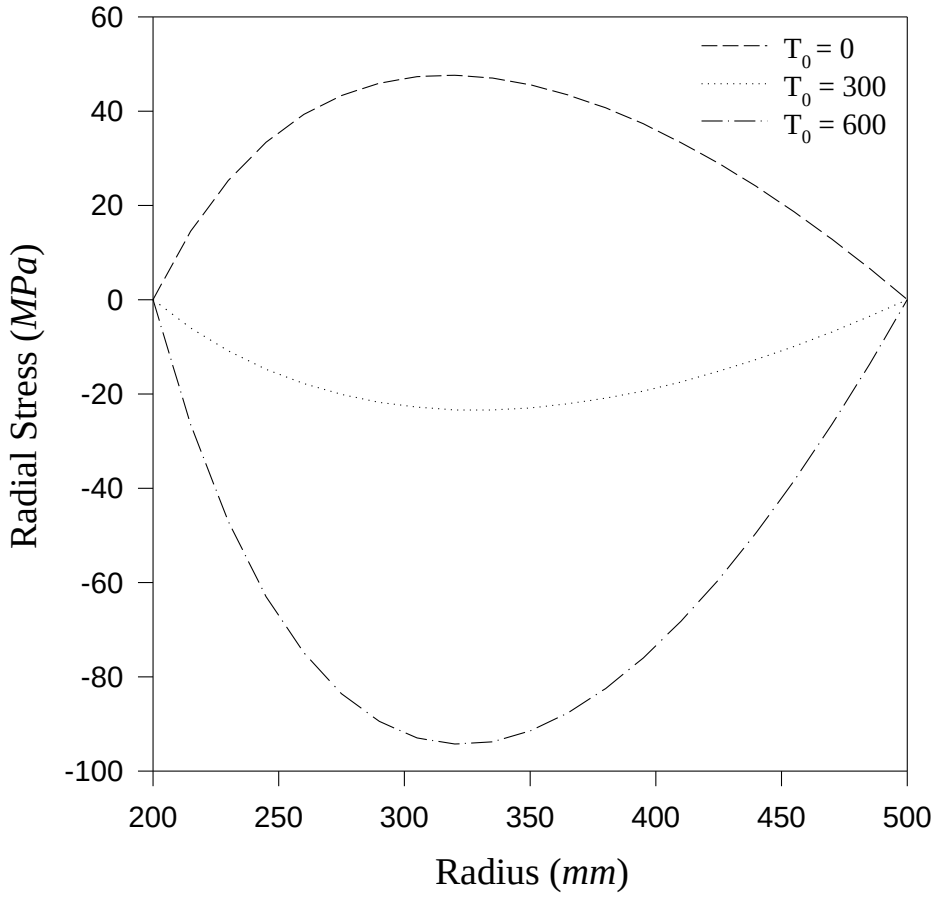

Figure 6.17 Variation of radial stress along radius with varying temperature.

The tangential strain rate, Figure 6.18, is least at the inner radius of the disc with increase in temperature, while moving towards the outer radius of the disc the value of tangential strain rate is increasing with increase in temperature and it is noticed as maximum at 600ºC. For lower temperature, the tangential strain rate changes from 1.51×10^{-3} s^{-1} to 5.69×10^{-4} s^{-1}, respectively, inner to outer radius. For higher temperature, it changes from 9.40×10^{-5} s^{-1} to 6.61×10^{-3} s^{-1}, respectively, inner to outer radius. The tangential strain rate almost remains same somewhere around radius 245 mm.

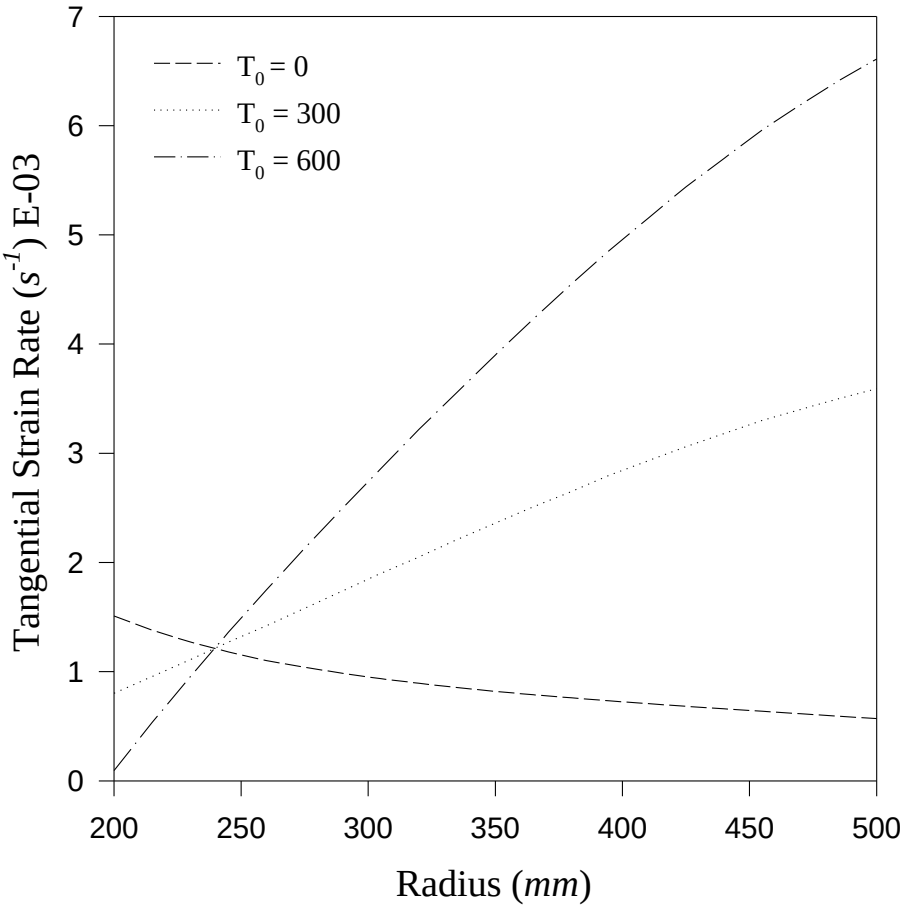

Figure 6.18 Variation of tangential strain rate along radius with varying temperature.

Figure 6.19 illustrates the effect of the temperature on radial strain rate with radius. It can be seen from the figure that there is very small variation in the radial strain rate for the disc when operated at 0ºC. At T_0= 300ºC and 600ºC, it is observed as tensile at most of the radii of the disc and compressive near outer radius of the disc. For the disc operating at temperature 0ºC, the radial strain rate changes from -4.53 × 10^{-4} s^{-1} to -1.71 × 10^{-4} s^{-1}, from inner to outer radius and for temperature 600ºC, it changes from 2.65 × 10^{-3} s^{-1} to -1.98 × 10^{-3} s^{-1}, from inner to outer radius. The radial strain rate almost remains same somewhere around radius 245 mm.

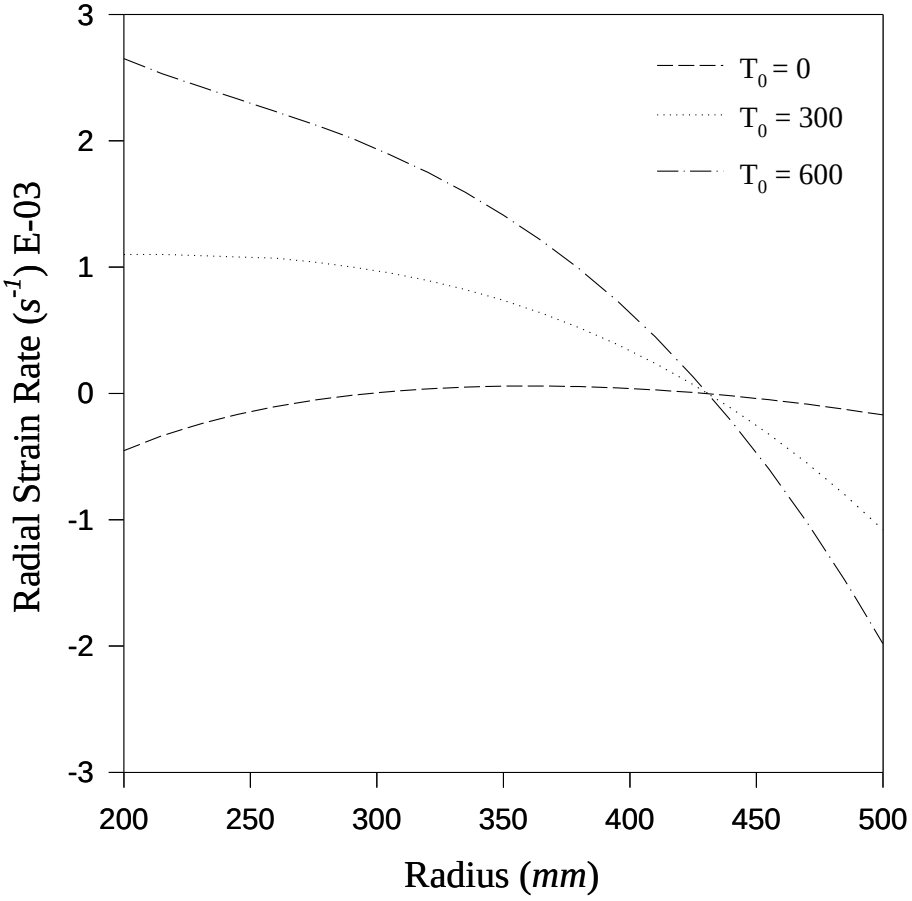

Figure 6.19 Variation of radial strain rate along radius with varying temperature.

Figure 6.20 shows the variation of radial displacement along the radial direction. For lower temperature, the value of radial displacement is noticed minimum from inner to outer radius of the disc and maximum for higher temperature. The maximum variation in radial displacement, corresponding to T_0= 600ºC and to T_0= 0ºC, is noticed around 1.368 mm and 3.015 mm, respectively, at the inner and outer radius of the disc.

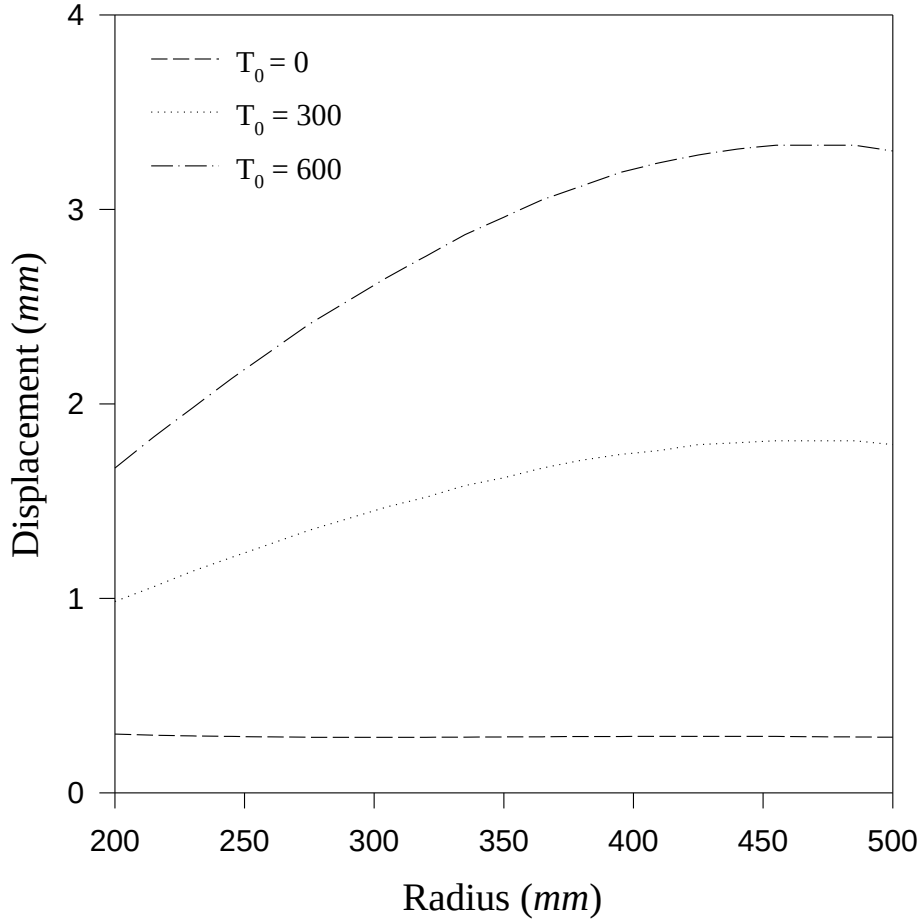

Figure 6.20 Variation of radial displacement along radius with varying temperature.

6.5 EFFECT OF AN INTERNAL PRESSURE

In this subsection, the effect of the internal pressure (p_i) on stresses, strain rates and displacement has been illustrated in Figures (6.21)-(6.25). To see this effect only Disc-3 is considered with two different cases:

(i) **Case-1**: Disc is rotating **without** internal pressure i.e. p_i = **0 MPa**

(ii) **Case-2**: Disc is rotating **with** internal pressure of p_i = **25 MPa.**

The material properties such as Young's modulus, density and thermal expansion coefficient, grading index, dimensions of disc and particle content of Disc-3 are given in Tables (2)-(5) of the *Appendix*.

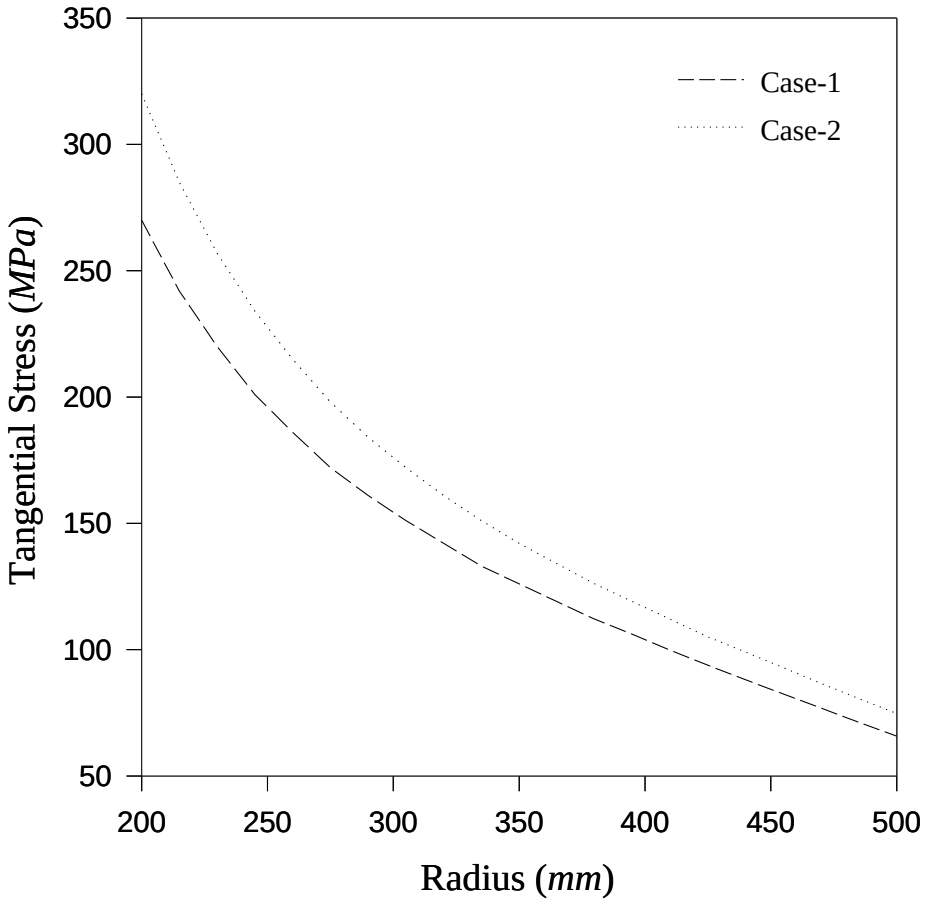

Figure 6.21 Effect of internal pressure on tangential stress.

Figure 6.21 shows the effect of internal pressure on the rotating disc along radial direction. It can be seen from the figure that the tangential stress is observed maximum throughout the disc for Case-2 when compared with Case-1. The maximum variation in the magnitude of tangential stress is observed at the inner radius (50 MPa), is noticed minimum at outer radius (9 MPa)

The variation of radial stress along the radial distance due to internal pressure is given in Figure 6.22. At the inner radius of the disc, it is noticed that the radial stress is equal to internal pressure for both cases and at the outer radius the radial stress is observed as zero for Case-1 as well as Case-2.

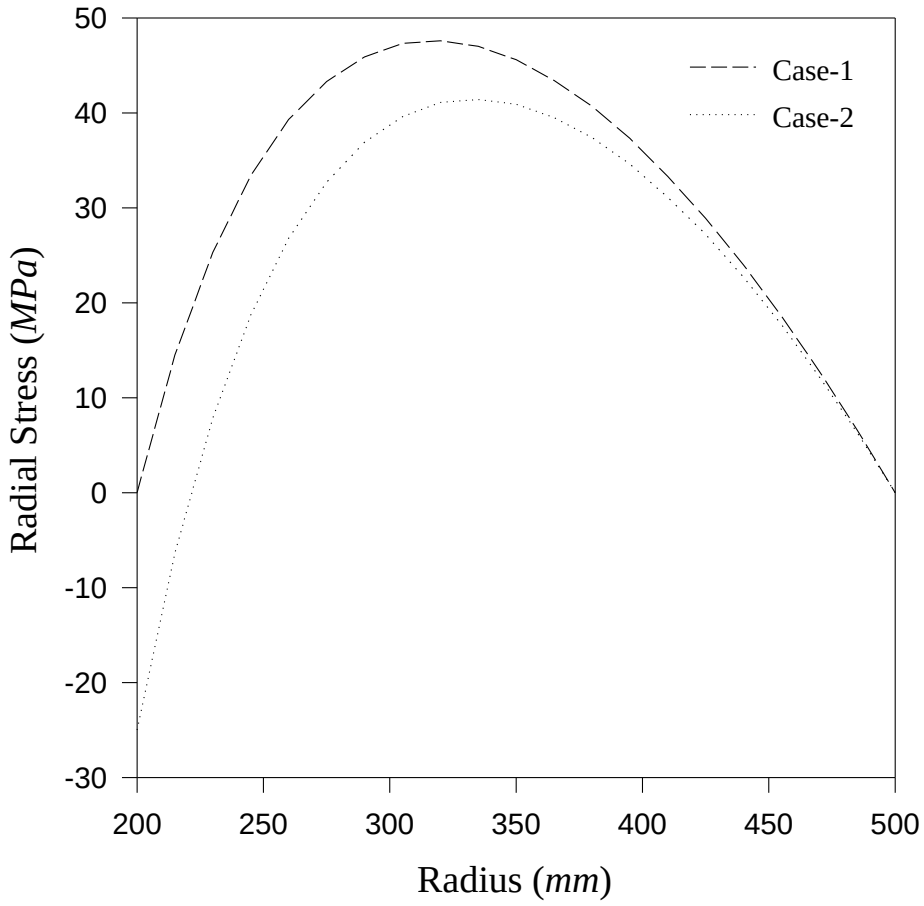

Figure 6.22 Effect of internal pressure on radial stress.

Figure 6.23 illustrates the effect of internal pressure on tangential strain rate along radius. It can be seen that throughout the disc, the tangential strain rate is maximum for Case-2 and minimum for Case-1. The decreasing trend is observed from inner to outer radius for both cases. For Case-2 the tangential strain rate changes from 1.83×10^{-3} s^{-1} to 6.47×10^{-4} s^{-1}, respectively, inner to outer radius and for Case-1, it changes from 1.51×10^{-3} s^{-1} to 5.69×10^{-4} s^{-1}, respectively, inner to outer radius of the disc.

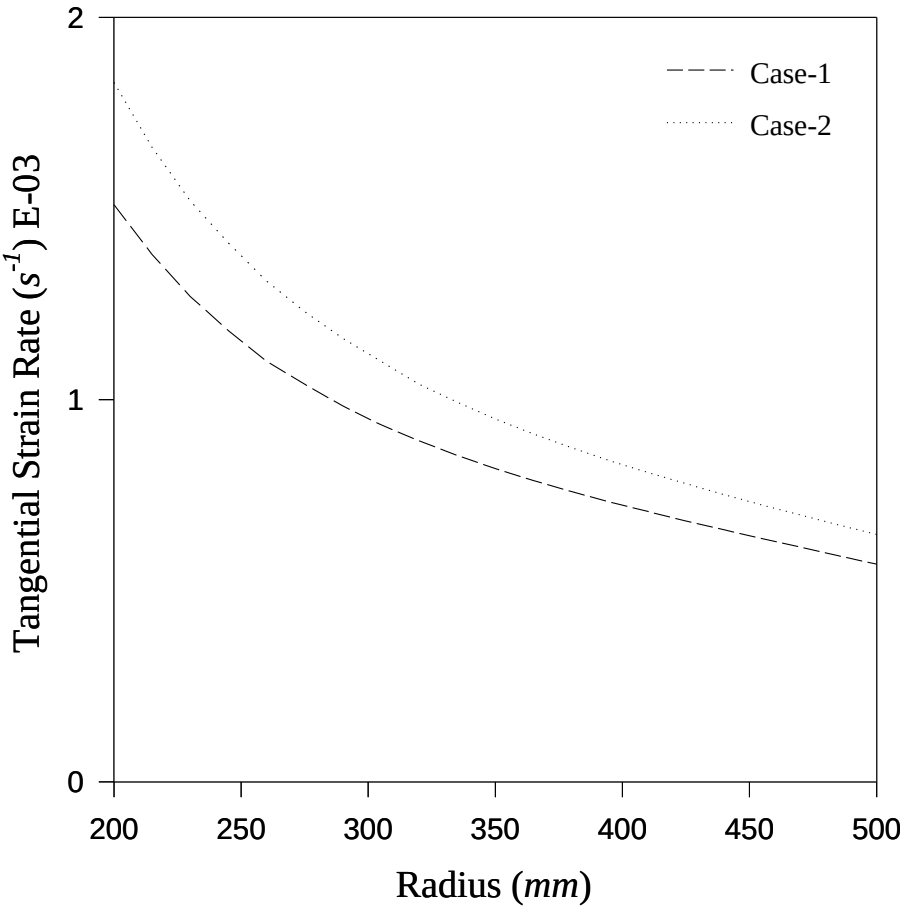

Figure 6.23 Effect of internal pressure on tangential strain rate.

The variation of radial strain rate along the radial distance due to internal pressure is shown in Figure 6.24. For Case-1, it can be seen from the figure that the radial strain rate is observed compressive at the inner and outer radius while it is becomes tensile in the middle region of the disc. Radial strain rate is noticed compressive over the entire radius of the disc for Case-2. The radial strain rate, for Case-2, is observed highest throughout the entire radius of the disc, while least for Case-1.

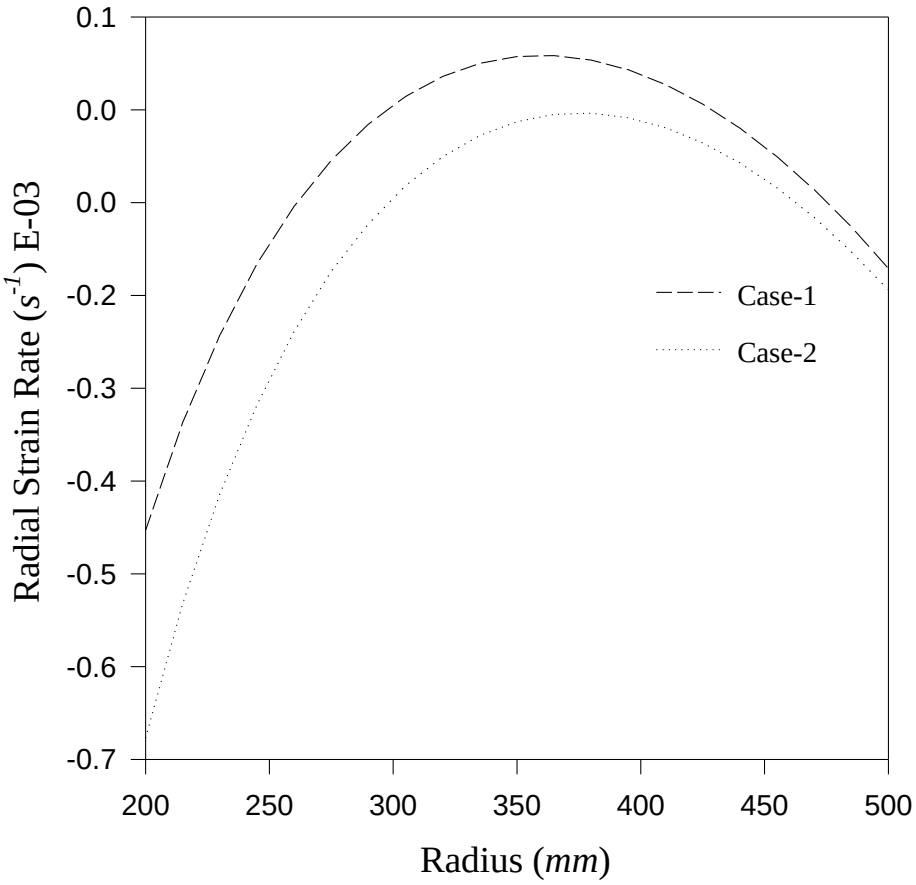

Figure 6.24 Effect of internal pressure on radial strain rate.

The effect of the internal pressure on radial displacement along radius is shown in Figure 6.25. The Figure reveals that the value of radial displacement is noticed minimum from inner to outer radius for Case-1 when compared with Case-2. The maximum variation in radial displacement, corresponding to Case-2 and Case-1, is noticed around 0.065 mm and 0.038 mm, respectively, at the inner and outer radius of the disc.

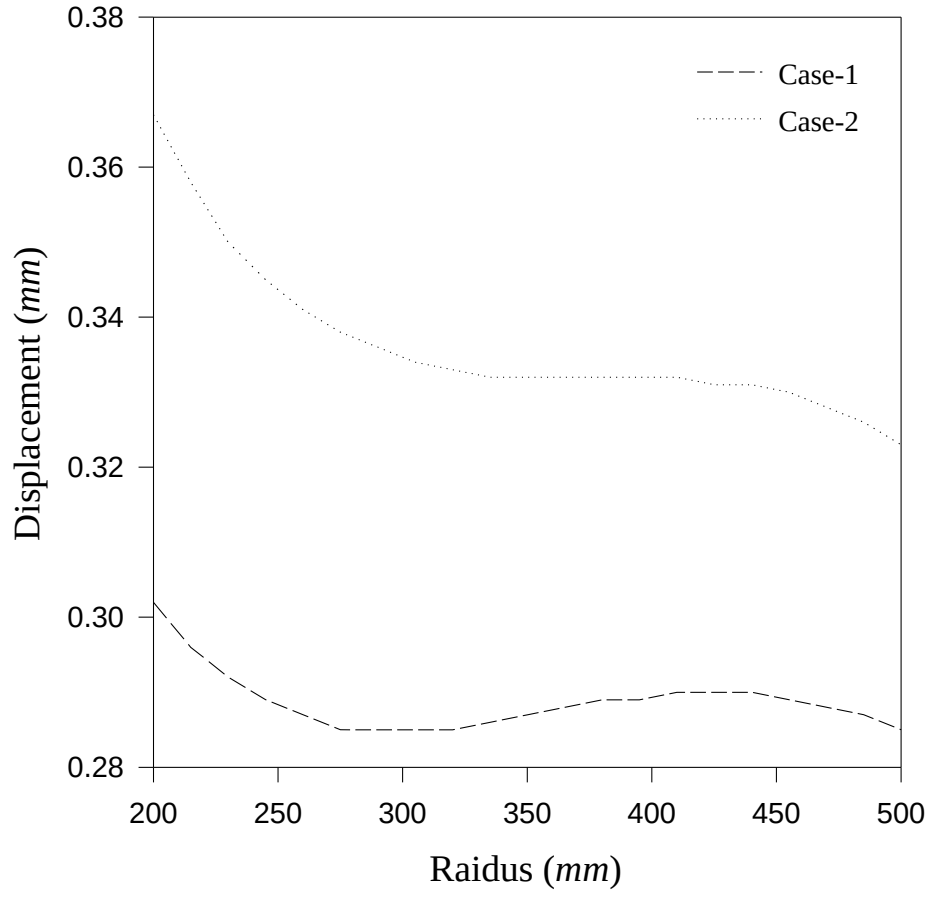

Figure 6.25 Effect of internal pressure on radial displacement.

CHAPTER 7
CONCLUSIONS

Based on the results obtained, some observations from the present research work can be summarized as follows:

(i) By increasing particle content in the discs, the tangential stress near the inner radius increases but decreases towards the outer radius. The magnitude of radial stress is found increasing with increase in particle content. Although, the tangential stress increases with increase in particle content at the inner radius but strain rates and displacement observed lower.

(ii) The tangential, radial stress, tangential strain rate and radial displacement values are noticed significantly lower in linearly varying thickness disc when compared with constant thickness disc.

(iii) By increasing the value of grading index (n), the tangential stress decreases at the inner radius while it increases at outer radius. Radial stress is observed to be decreasing with increase in n. Strain rates and displacement is noticed least for n = -0.5.

(iv) The tangential stress changes from compressive to tensile from inner to outer radius with increase in temperature whereas the radial stress decreases with increase in temperature. Tangential strain rate are maximum at inner radius but reduced at outer radius for 0ºC, while it is reversed with increase in temperature.

(v) Stresses, strain rates and displacement are observed to be increasing when disc is operated under internal pressure (p_i).

FUTURE SCOPE OF WORK

The present study carried out in this thesis may be further extended in the following directions:

(i) The response of stresses, strain rates and displacement may be investigated by repeating the analysis for other thickness as well as grading profiles.

(ii) Present study may also be carried out for other materials as well.

(iii) The study carried out in this research work may be extended for different temperature profiles.

(iv) The research problem may also be solved with other numerical method like Runge Kutta (RK) algorithm.

REFERENCES

[1] **Reddy, T.Y., and Shrinath, H., (1974),** "Elastic Stresses in a Rotating Anisotropic Annular Disc of Variable Thickness and Variable Density", *Internal Journal of Mechanical Sciences*, **16,** 85-89.

[2] **Goven, U., (1992),** "Elastic-Plastic Stresses in a Rotating Annular Disk of Variable Thickness and Variable Density", *Internal Journal of Mechanical Sciences*, **34,** 133-138.

[3] **Shukla, R.K., (1996),** "Creep Transition in a Thin Rotating Non-Homogeneous Disc", *Indian Journal of Pure and Applied Mathematics*, **27(5)**, 487-498.

[4] **Horgan, C.O., and Chan, A.M., (1999),** "The Stress Response of Functionally Graded Isotropic Linearly Elastic Rotating Disks", *Journal of Elasticity*, **55,** 219-230.

[5] **You, L.H., Tang, Y.Y., Zhang, J.J., and Zheng, C.Y., (2000),** "Numerical Analysis of Elastic-Plastic Rotating Disks with Arbitrary Variable Thickness and Density", *International Journal of Solids and Structures*, **37,** 7809-7820.

[6] **Eraslan, A.N., and Orcan, Y., (2002),** "Elastic-Plastic Deformation of a Rotating Solid Disk of Exponentially Varying Thickness", *Mechanics of Materials*, **34,** 423-432.

[7] **Singh, S.B., and Ray, S., (2003),** "Creep Analysis in an Isotropic FGM Rotating Disc of Al-SiC Composite", *Journal of Materials Processing Technology*, **143-144,** 616–622.

[8] **Callioglu, H., (2004),** "Stress Analysis of an Orthotropic Rotating Disc under Thermal Loading", *Journal of Reinforced Plastics and Composites*, **23,** 1859-1867.

[9] **Callioglu, H., Topcu, M., and Tarakcilar, A.R., (2006),** "Elastic-Plastic Stress Analysis of an Orthotropic Rotating Disc", *International Journal of Mechanical Sciences*, **48,** 985-990.

[10] **Eraslan, A.N., and Akis, T., (2006),** "On the Plane Strain and Plane Stress Solutions of Functionally Graded Rotating Solid Shaft and Solid Disk Problems", *Acta Mechanica*, **181,** 43-63.

[11] **Witek, L., (2006),** "Failure Analysis of Turbine Disc of an Aero Engine", *Engineering Failure Analysis*, **13,** 9-17.

[12] **Bayat, M., Saleem, M., Sahari, B.B., Hamouda, A.M.S., and Mahdi, E., (2007),** "Thermo Elastic Analysis of a Functionally Graded Rotating Disk with Small and Large Deflections", *Thin Walled Structures*, **45,** 677-691.

[13] **You, L.H., You, X.Y., Zhang, J.J., and Li, J., (2007),** "On Rotating Circular Discs with Varying Material Properties", *Zeitschrift fur Angewandte Mathematik und Physik*, **58**, 1068-1084.

[14] **Altan, G., Topcu, M., Bektas, N.B., and Altan, B.D., (2008),** "Elastic-Plastic Thermal Stress Analysis of an Aluminum Composite Disc under Parabolic Thermal Load Distribution", *Journal of Mechanical Science and Technology*, **22,** 2318-2327.

[15] **Bayat, M., Saleem, M., Sahari, B.B., Hamouda, A.M.S., and Mahdi, E., (2008),** "Analysis of Functionally Graded Rotating Disks with Variable Thickness", *Mechanics Research Communications*, **35,** 283-309.

[16] **Hojjati, M.H., and Hassani, A., (2008),** "Theoretical and Numerical Analyses of Rotating Discs of Non-Uniform Thickness and Density", *International Journal of Pressure Vessels and Piping*, **85,** 694-700.

[17] **Pankaj (2009),** "Elastic-Plastic Transition Stresses in an Isotropic Disc having Variable Thickness Subjected to Internal Pressure", *International Journal of Physical Sciences*, **4(5)**, 336-342.

[18] **Zenkour, A.M., (2009),** "Stress Distribution in Rotating Composite Structures of Functionally Graded Solid Disks", *Journal of Materials Processing Technology*, **209,** 3511-3517.

[19] **Afsar, A.M., and Go, J., (2010),** "Finite Element Analysis of Thermoelastic Field in a Rotating FGM Circular Disk", *Applied Mathematical Modelling*, **34,** 3309-3320.

[20] **Callioglu, H., (2010),** "Stress Analysis in a Functionally Graded Disc under Mechanical and Thermal Loads and a Steady State Temperature Distribution", *Indian Academy of Sciences*, **36,** 53-64.

[21] **Deepak, D., Gupta, V.K., and Dham, A.K., (2010),** "Creep Modeling in Functionally Graded Rotating Disc of Variable Thickness", *Journal of Mechanical Science and Technology*, **24,** 1-12.

[22] **Rattan, M., Chamol, N., and Singh, S.B., (2010),** "Creep Analysis of an Isotropic Functionally Graded Rotating Disc", *International Journal of Contemporary Mathematical Sciences*, **5**, 419-431.

[23] **Callioglu, H., Sayer, M., and Demir, E., (2011),** "Stress Analysis of Functionally Graded Discs under Mechanical and Thermal Loads", *Indian Journal of Engineering and Material Sciences*, **18,** 111-118.

[24] **EkhteraeiToussi, H., and RezaeiFarimani, M., (2011),** "Elasto-Plastic Deformation Analysis of Rotating Disc Beyond its Limit Speed", *International Journal of Pressure Vessels and Piping*, **89,** 170-177.

[25] **Loghman, A., Arani, A.G., Shajari, A.R., and Amir, S., (2011),** "Time-Dependent Thermoelastic Creep Analysis of Rotating Disk Made of Al-SiC Composite", *Archive of Applied Mechanics*, **81,** 1853-1864.

[26] **Hassani, A., Hojjati, M.H., Farrahi, G.H., and Alashti, R.A., (2012),** "Semi-Exact Solution for Thermo Mechanical Analysis of Functionally Graded Elastic Strain Hardening Rotating disks", *Communications in Nonlinear Science and Numerical Simulation*, **17,** 3747-3762.

[27] **Kansal, G., and Parvez, M., (2012),** "Thermal Stress Analysis of Orthotropic Graded Rotating Discs", *International Journal of Modern Engineering Research*, **2,** 3881-3885.

[28] **Mahamood, R.M., (2012),** "Functionally Graded Material: An Overview", *Proceedings of the World Congress on Engineering*, **3.**

[29] **Sharma, J.N., Sharma, D., and Kumar, S., (2012),** "Stress and Strain Analysis of Rotating FGM Thermoelastic Circular Disk by Using FEM", *International Journal of Pure Applied Mathematics*, **74,** 339-352.

[30] **Garg, M., Salaria, B.S., and Gupta, V.K., (2013),** "Effect of Thermal Gradient on Steady State Creep in a Rotating Disc of Variable thickness", *Procedia Engineering*, **55,** 542-547.

[31] **Shahzamanian, M.M., Sahari, B.B., Bayat, M., Mustapha, F., and Ismarrubie, Z.N., (2013),** "Elastic Contact Analysis of Functionally Graded Brake Disks Subjected to Thermal and Mechanical Loads", *International Journal for Computational Methods in Engineering Science and Mechanics*, **14,** 10-23.

TEXT REFERENCES

[32] **Kaw, A.K., (1997),** "Mechanics of Composite Materials", *CRC Press, America*, 2-18.

[33] **Chung, D.D.L., (2003),** "Composite Materials Science and Application", *Springer London,* 1-26.

WEB REFERENCES

[34] http://www.redwoodhikes.com/RNP/TallTrees.html
(Downloaded on November 19, 2012)

[35] http://composite-beams.beamss.info/concrete-beam/
(Downloaded on November 19, 2012)

[36] http://nptel.iitm.ac.in/courses/Webcourse-contents/IISc-BANG/Composite%20Materials/pdf/Teacher_Slides/mod1.pdf
(Downloaded on April 13, 2013)

APPENDIX

Table 1: Dimensions, material properties and operating conditions for validation [23]

Dimensions and Material Properties for the Rotating Disc	Inner Radius (a) = 200 mm Outer Radius (b) = 500 mm Disc Thickness (t) = 5 mm Thickness Gradient (k) = 0 Poisson's Ratio (v) = 0.3 Grading Index(n) = n_1 = -0.5194, n_2 = -0.4873 and n_3= 0.5236 Young's Modulus $E(r)$ = 150 GPa Density of the Disc Material $\rho(r)$ = 5600 kg/m^3 Thermal expansion coefficient $\alpha(r)$ = 23×10^{-6} 1/ºC
Operating Conditions for Rotating Disc	Disc Speed (ω)= 650 rad/sec Operating Temperature T_0 = 0ºC Internal Pressure (p_i) = 0

Table 2: Material properties for discs

Material Properties	Particle Contents (Vol. %)		
	20%	25%	30%
Young's Modulus $E(r)$ GPa	138	126.151	115.426
Density of the Disc Material $\rho(r)$ kg/m^3	2800	2781.747	2763.513
Thermal expansion coefficient $\alpha(r)$ 1/ºC	1.928 E-05	1.993 E-05	2.074 E-05

Table 3: Grading index for different particle content

Grading Index (n)	Particle Contents (Vol. %)		
	20%	25%	30%
n_1	0	-0.245	-0.477
n_2	0	-0.018	-0.036
n_3	0	0.103	0.207

Table 4: Dimensions and other parameters of discs

Dimensions and other Parameters	Inner Radius (a) = 200 mm Outer Radius (b) = 500 mm Disc Thickness (t) = 5 mm Poisson's Ratio (v) = 0.3 Thickness Gradient (k) = -0.5
Operating Conditions	Disc Speed (ω)= 650 rad/sec Operating Temperature T_0 = 0ºC Internal Pressure (p_i) = 0

Table 5: Particle content for three discs

Disc Notations	Particle Content (Vol. %)		
	V_{max}	V_{min}	V_{avg}
Disc-1	20	20	20
Disc-2	25	15.681	20
Disc-3	30	11.362	20

Table 6: Material properties and operating conditions of disc

Material Properties	Thickness Gradient (k)		
	k = 0	k = -0.2	k = -0.4
Young's Modulus $E(r)$ GPa	124.639	124.501	124.370
Density of the Disc Material $\rho(r)$ kg/m^3	2779.063	2778.933	2778.809
Thermal expansion coefficient $\alpha(r)$ 1/ºC	2.010 E-05	2.010 E-05	2.011 E-05

Table 7: Grading index for different values of thickness gradient

Grading Index (n)	Thickness Gradient (k)		
	k = 0	k = -0.2	k = -0.4
n_1	-0.302	-0.294	-0.286
n_2	-0.228	-0.022	-0.021
n_3	0.129	0.125	0.121

Table 8: Particle content for different values of thickness gradient

Thickness Gradient (k)	Particle Content (Vol. %)		
	V_{max}	V_{min}	V_{avg}
k = 0	26.666	20	20
k = -0.2	26.304	15	20
k = -0.4	25.956	15	20